Detectors in Nuclear Physics:

Monte Carlo Methods

Dr Andrea Mairani

Lectures III-IV

Medical Applications

Radiotherapy/Ion Beam Therapy

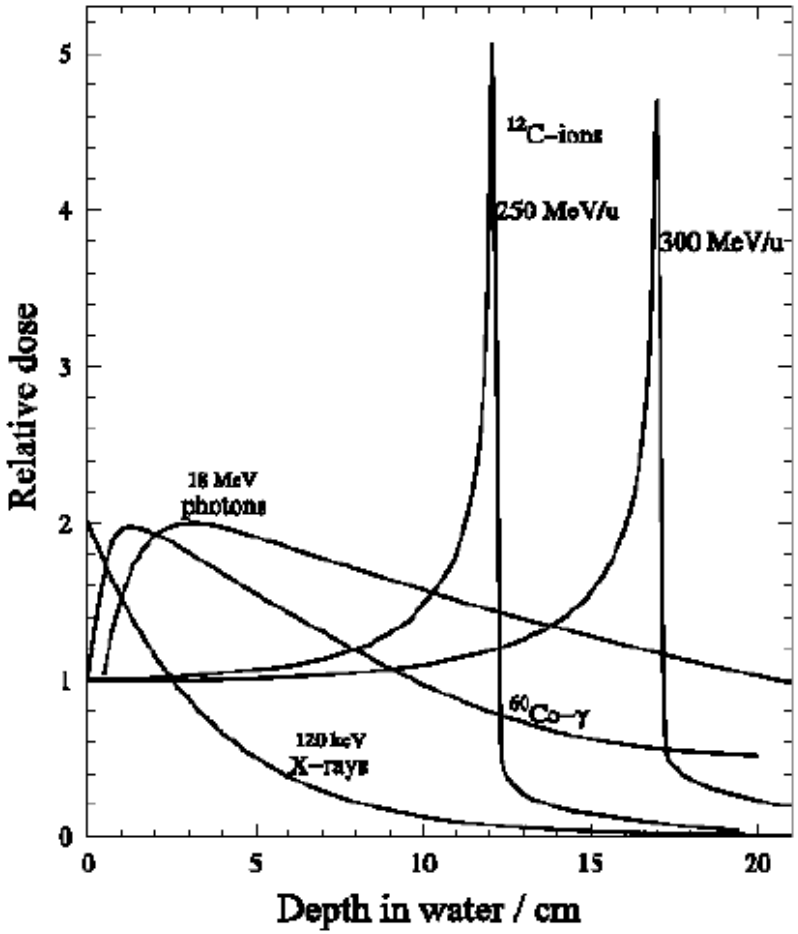

Figure 1.1: Dose depth profiles of photons from different radiation sources and carbon ions in water [24]. Variation of the ion energy allows the sharp dose maximum to be precisely located within the tumor.

In nuclear physics

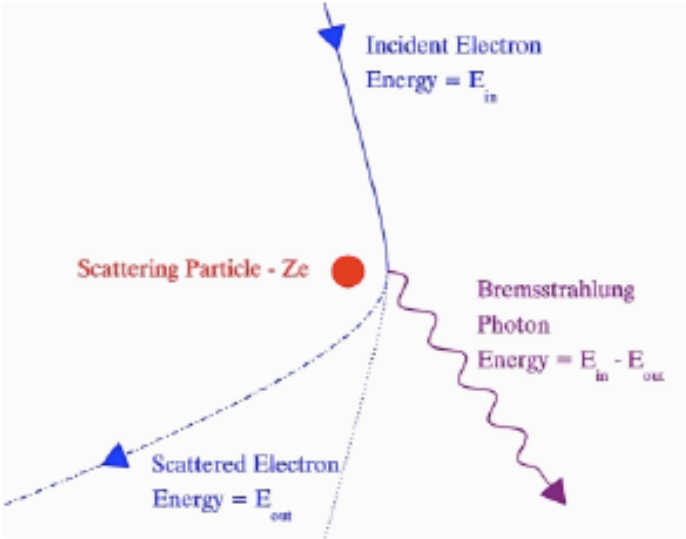

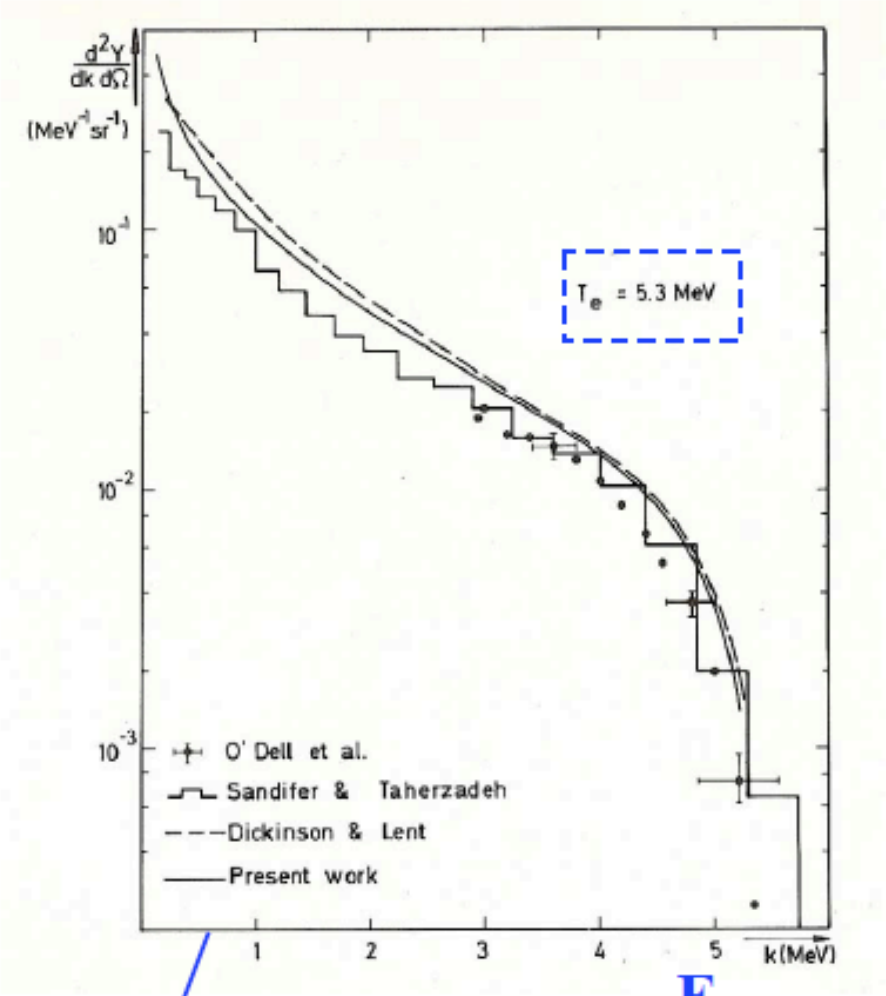

For typical electron energy the bremsstrahlung photon energy is quite low
⇒ it is reabsorbed close to its point of origin

Radiotherapy

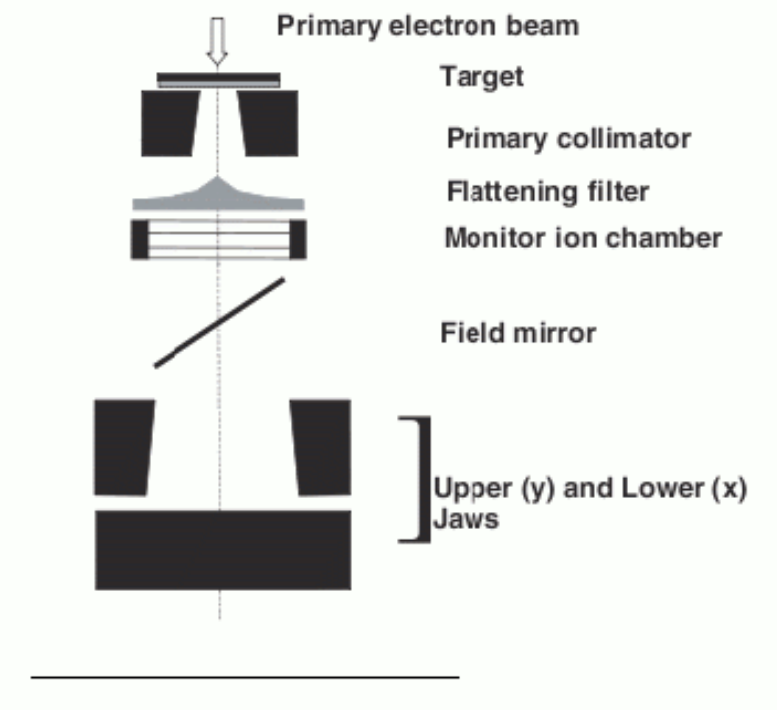

Figura 1.3: Rappresentazione schematica della testata radiante dell'acceleratore modellizzata nella simulazione Monte Carlo [8].

FLUKA radiotherapy simulation

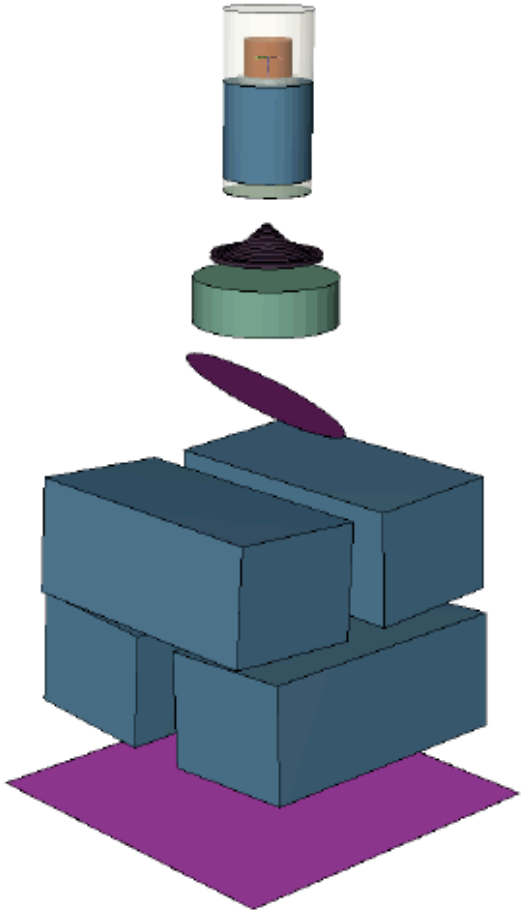

Figura 2.1: Rappresentazione della testata radiante dell'acceleratore utilizzata per la simulazione ottenuta mediante il programma SimpleGeo [12].

FLUKA radiotherapy simulation

Figura 2.2: Rappresentazione di alcuni componenti della testata radiante utilizzati nella simulazione: bersaglio, collimatore primario, finestra di berillio, filtro di appiattimento e camere monitor.

6 MeV Accelerator – electron fluence distribution

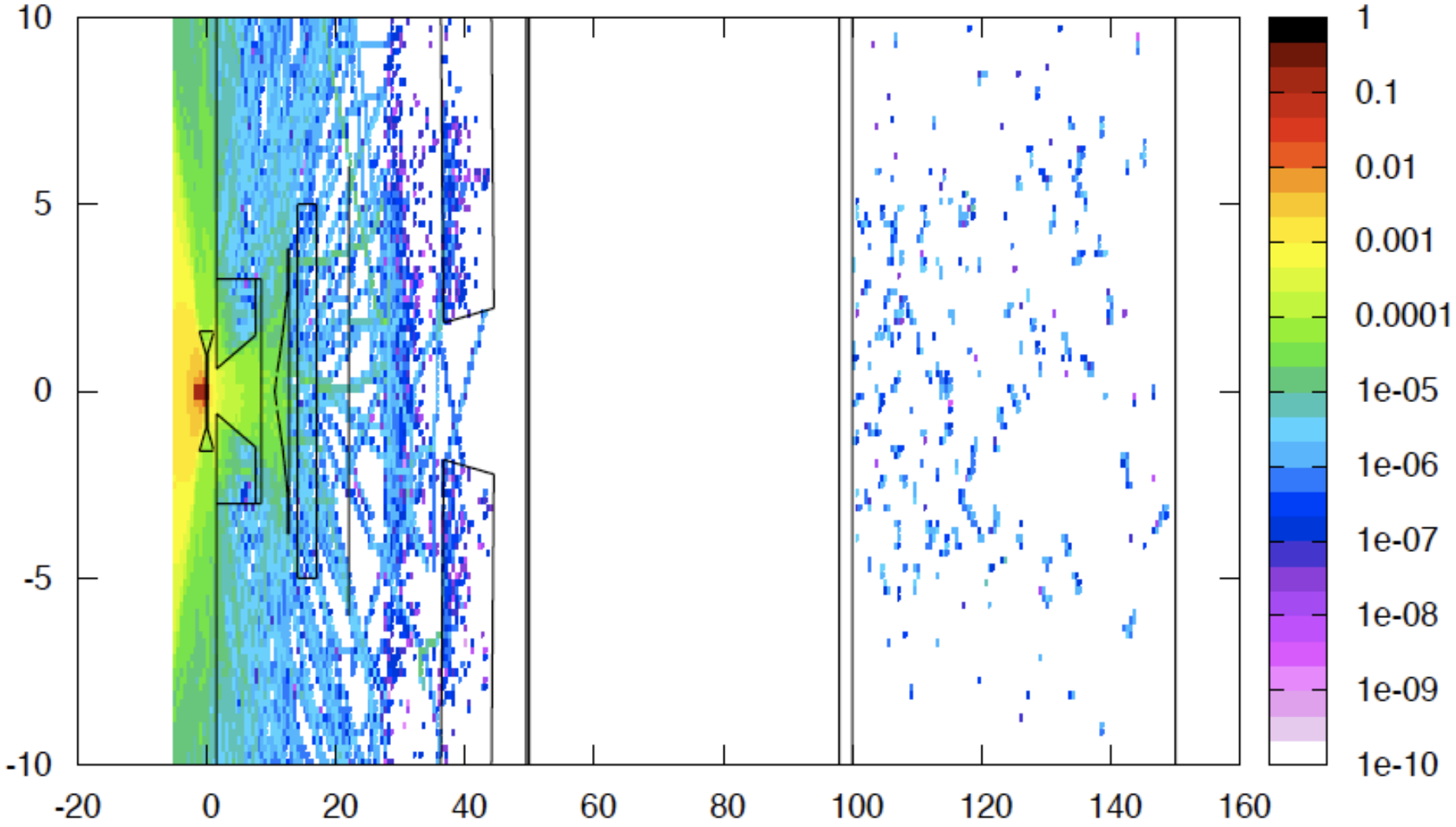

6 MeV Accelerator –photon fluence distribution

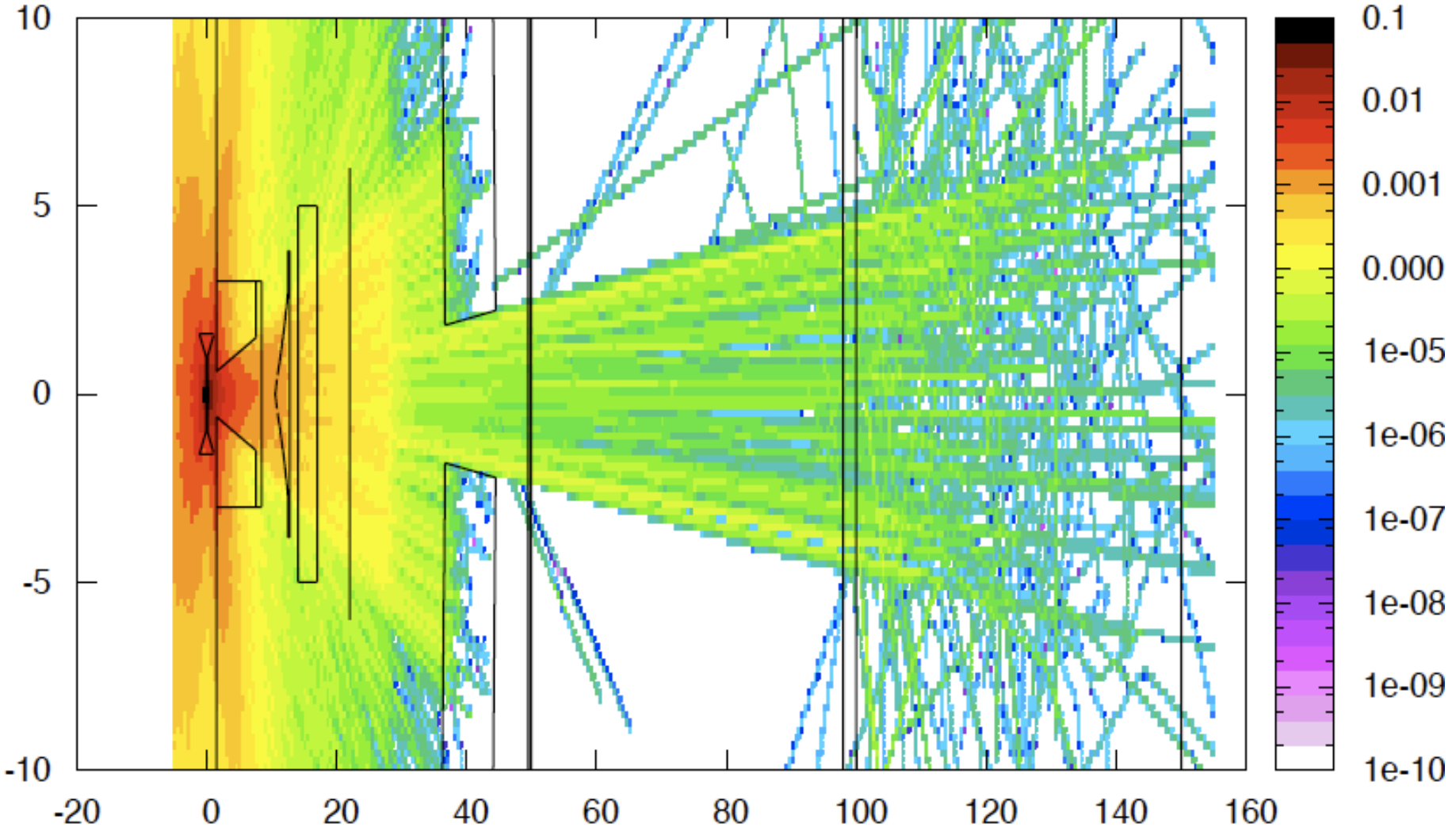

6 MeV Accelerator

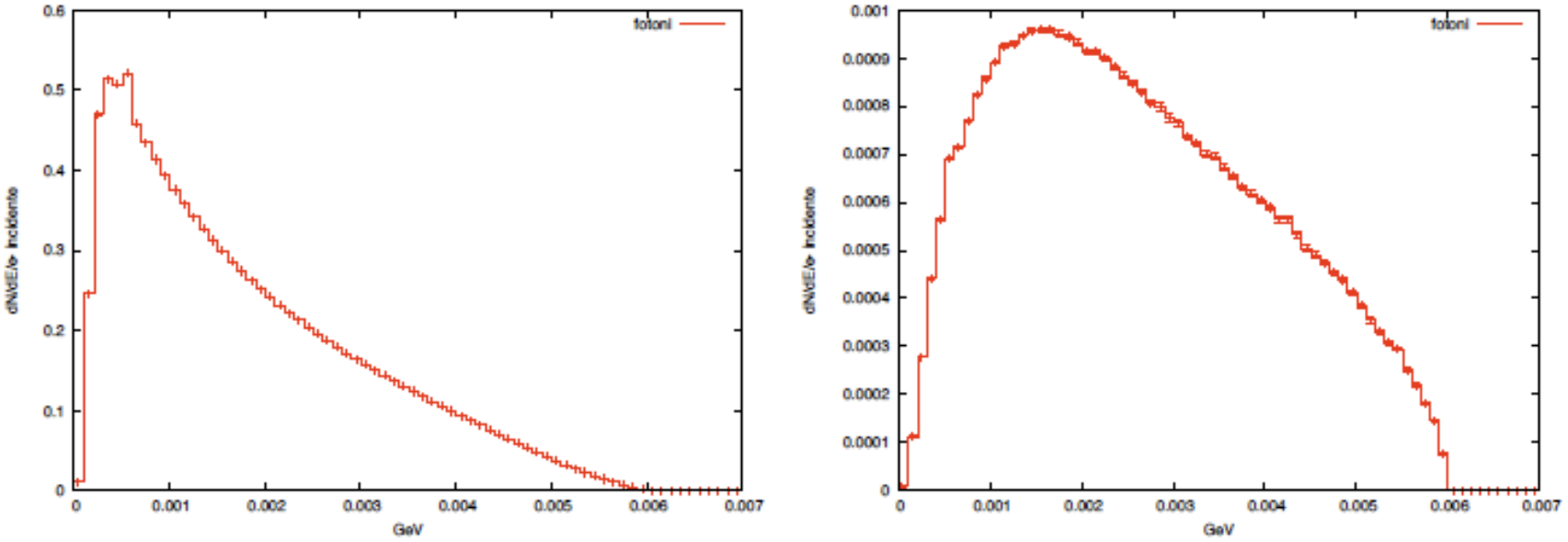

Figura 3.1: Spettri energetici dei fotoni emessi all'uscita del target (sinistra) e all'isocentro (destra).

6 MeV Accelerator

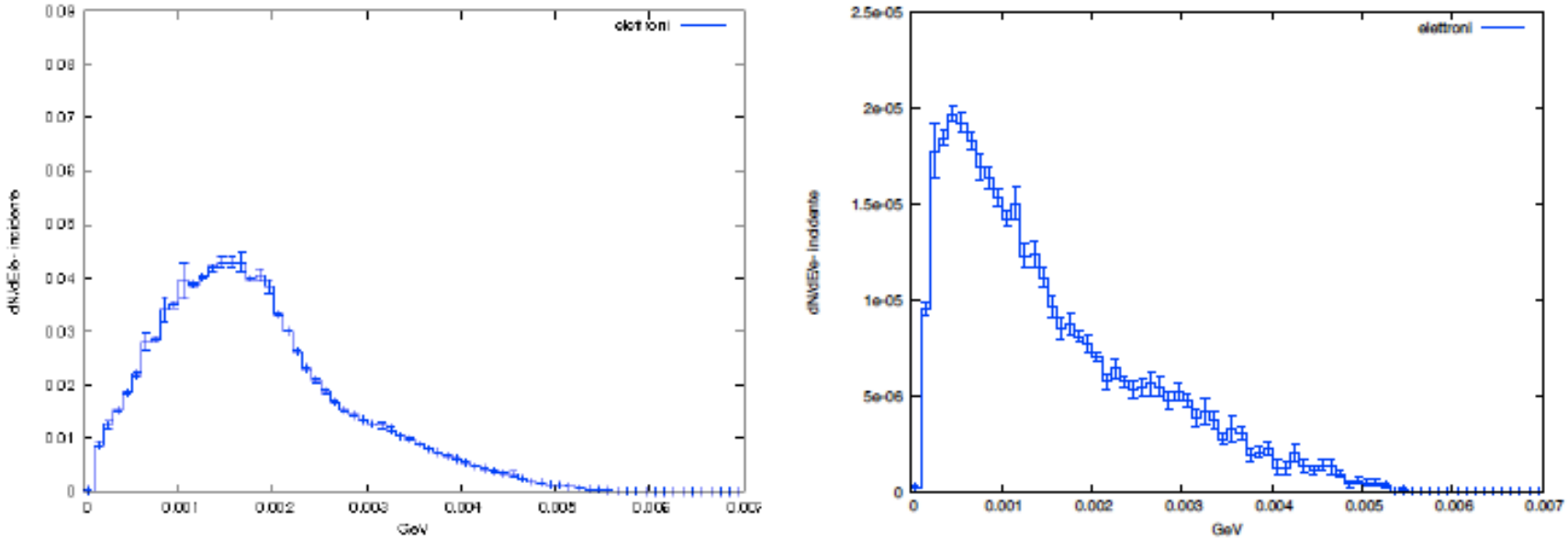

Figura 3.2: Spettri energetici degli elettroni emessi all'uscita del target (sinistra) e all'isocentro (destra).

6 MeV Accelerator

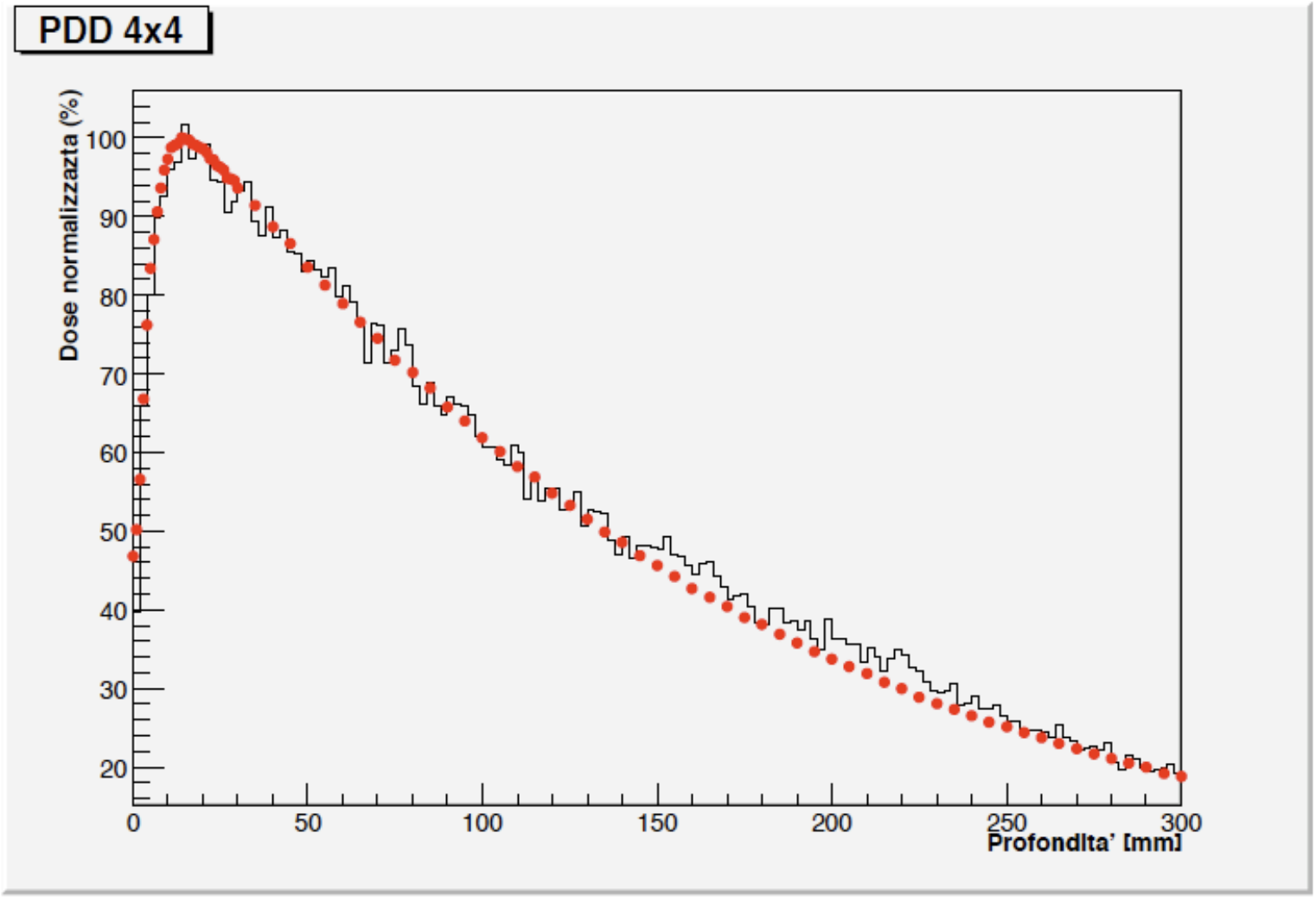

Figura 3.5: Curve di dose in profondità simulate con energia nominale pari a 6 MV; i pallini rossi sono le misure sperimentali e la linea nera rappresenta le simulazioni teoriche.

6 MeV Accelerator

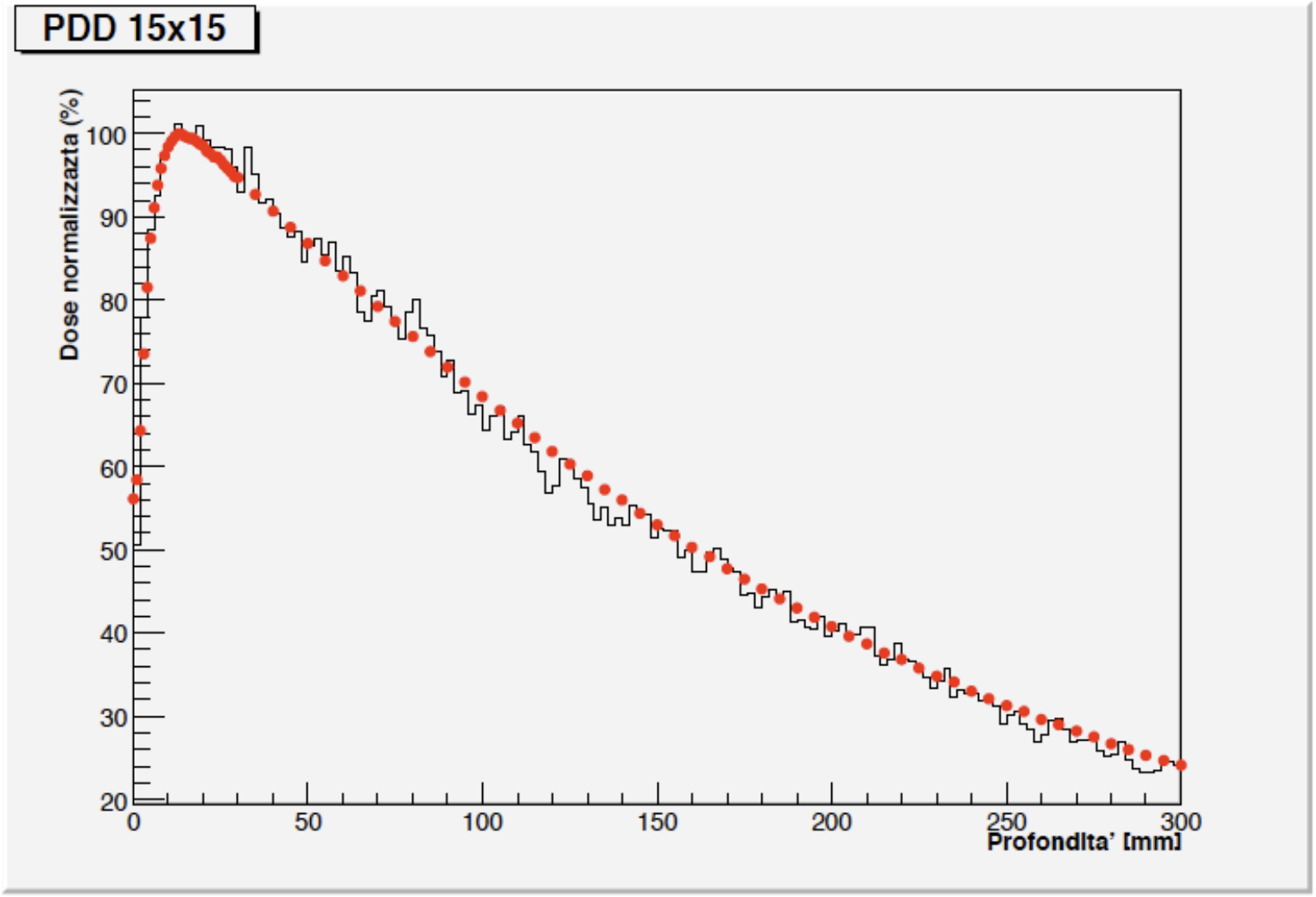

Figura 3.7: Curve di dose in profondità simulate con energia nominale pari a 6 MV; i pallini rossi sono le misure sperimentali e la linea nera rappresenta le simulazioni teoriche.

6 MeV Accelerator

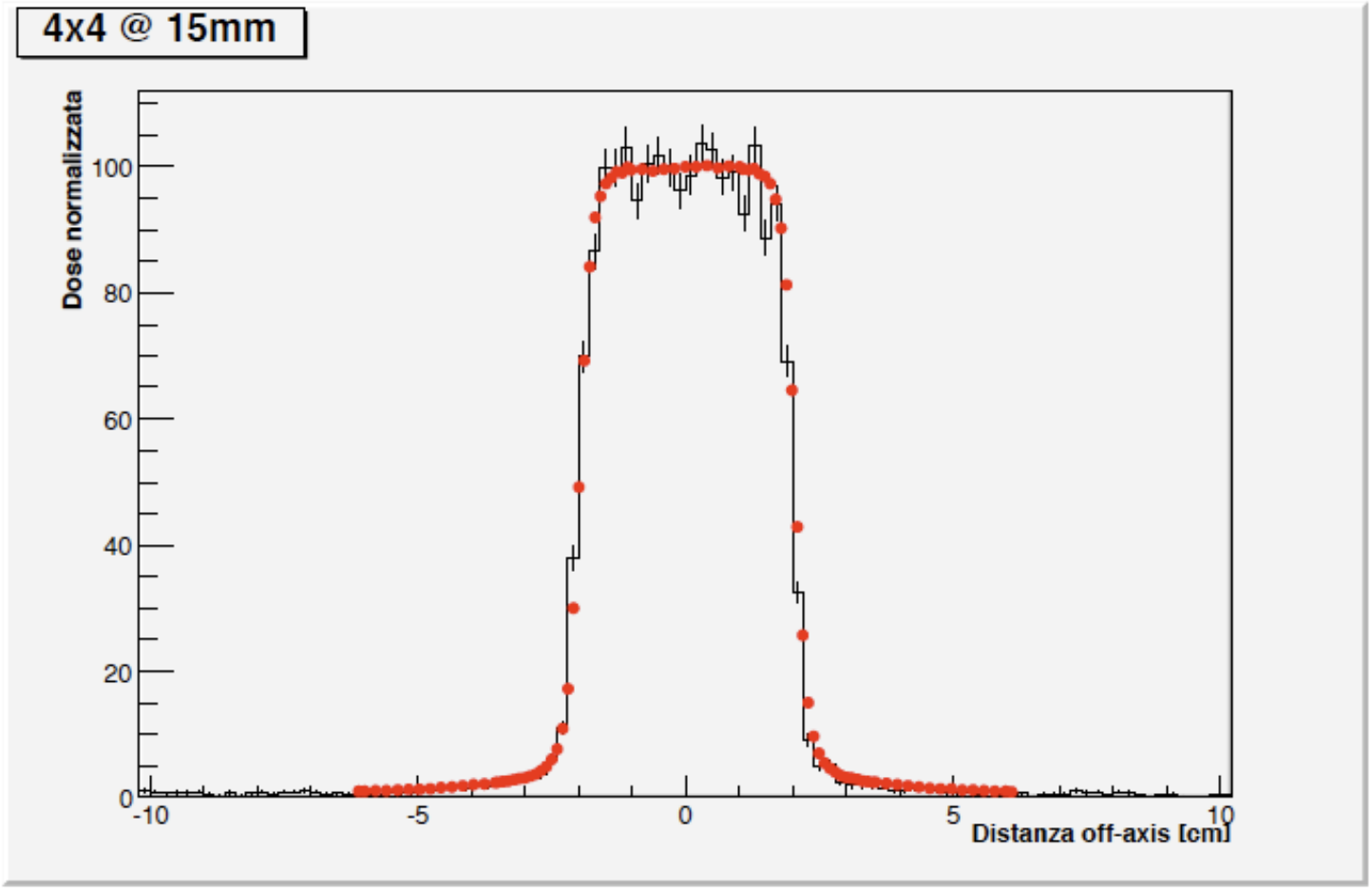

Figura 3.9: Profili di dose sperimentali e teorici. I pallini rossi sono le misure sperimentali e la linea nera rappresenta le simulazioni teoriche.

6 MeV Accelerator

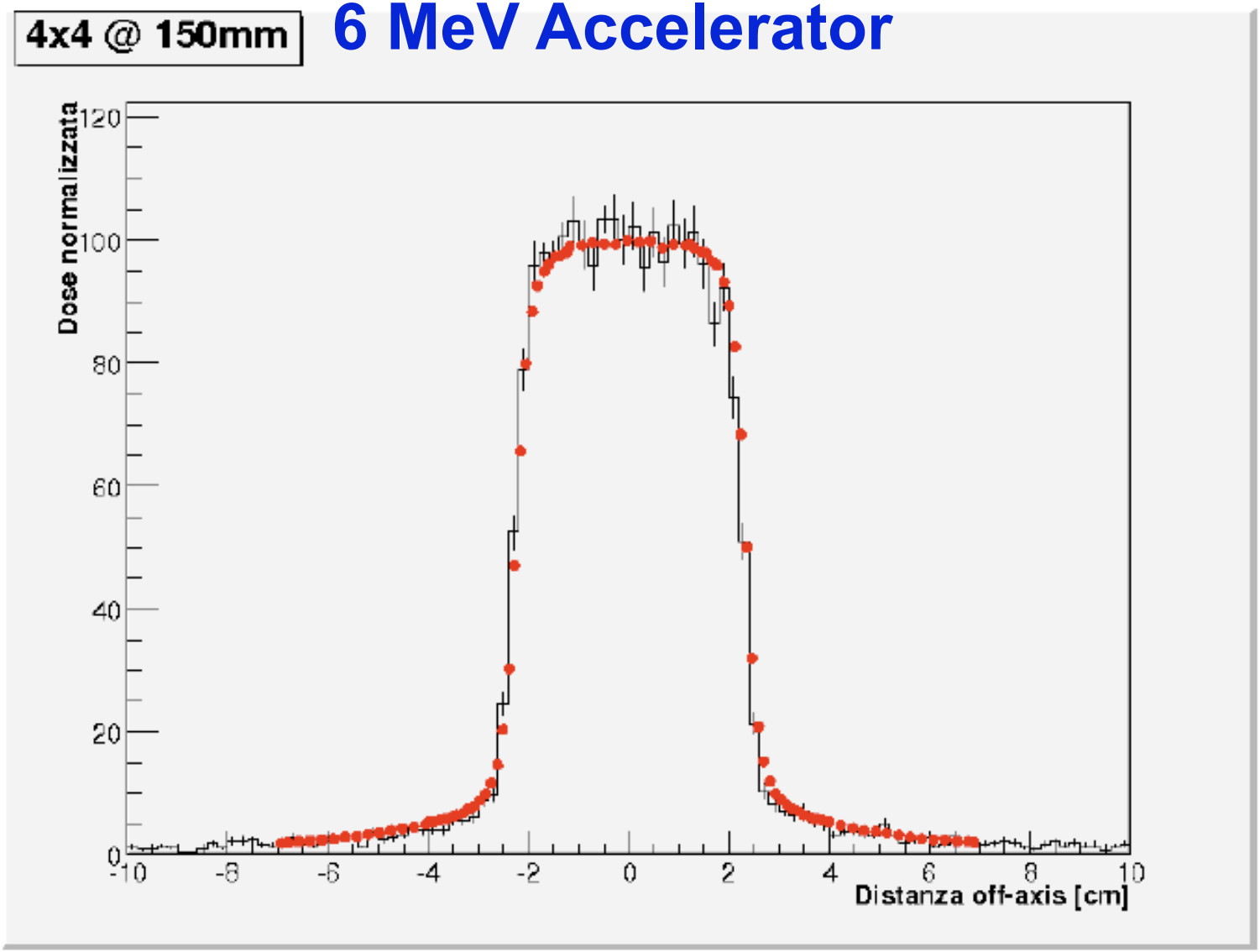

Figura 3.11: Profili di dose sperimentali e teorici. I pallini rossi sono le misure sperimentali e la linea nera rappresenta le simulazioni teoriche.

Mixed Radiation Field in Carbon Ion Therapy

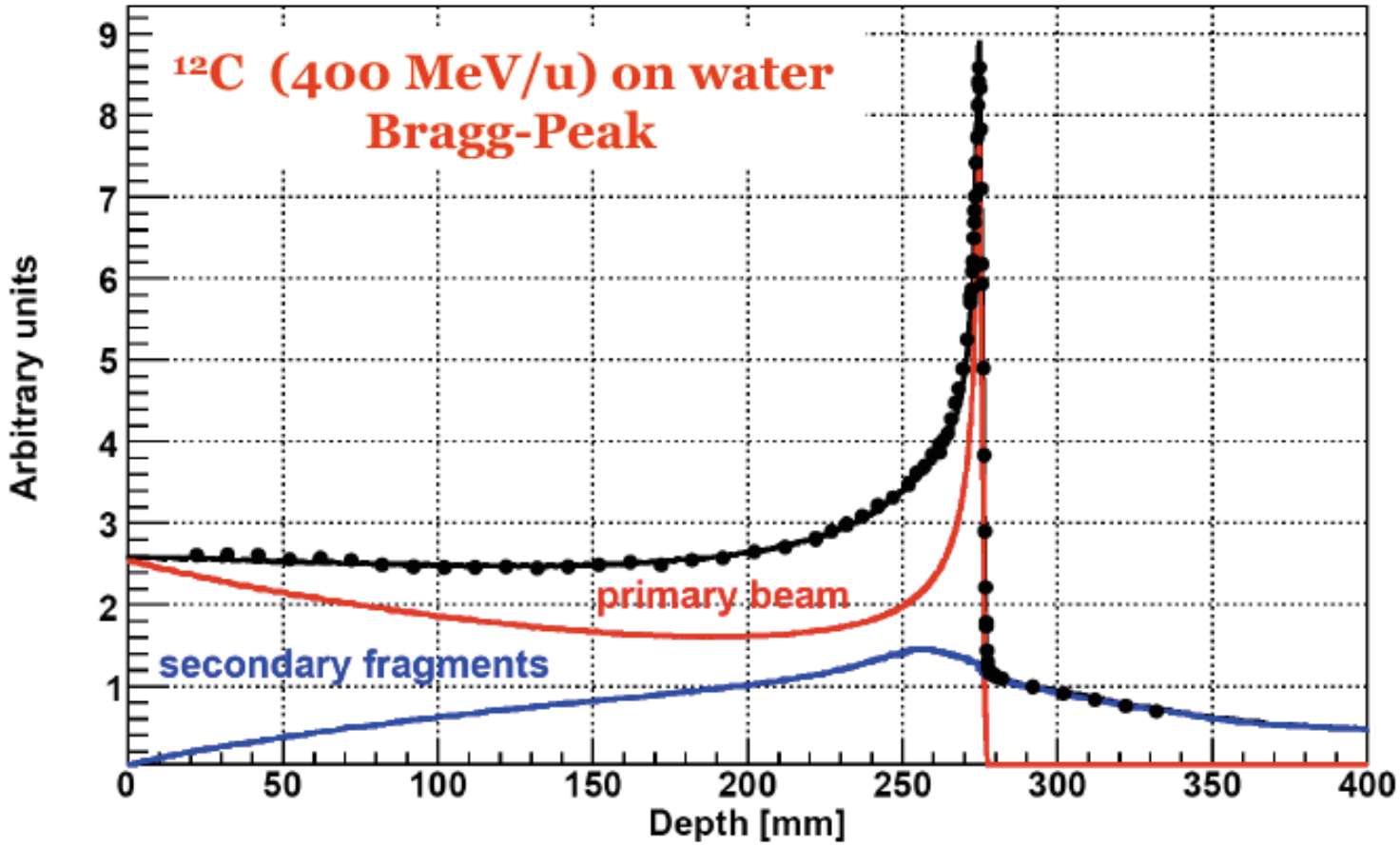

Exp. Data (points) from Haettner et al, Rad. Prot. Dos. 2006

Simulation: A. Mairani PhD Thesis, 2007, Nuovo Cimento C, 31, 2008

Nuclear Models

Heavy ion interaction models in FLUKA - 1

E > 5 GeV/n

Dual Parton Model (DPM)

DPMJET-III (original code by R.Engel, J.Ranft and S.Roesler, FLUKA-implemenation by T.Empl *et al.*)

0.1 GeV/n < E < 5 GeV/n

Relativistic Quantum Molecular Dynamics Model (RQMD)

RQMD-2.4 (original code by H.Sorge *et al.*, FLUKA-implementation by A.Ferrari *et al.*)

E < 0.1 GeV/n

Boltzmann Master Equation (BME) theory

BME (original code by E.Gadioli *et al.*, FLUKA-implementation by F.Cerutti *et al.*)

Heavy ion interaction models in FLUKA - 2

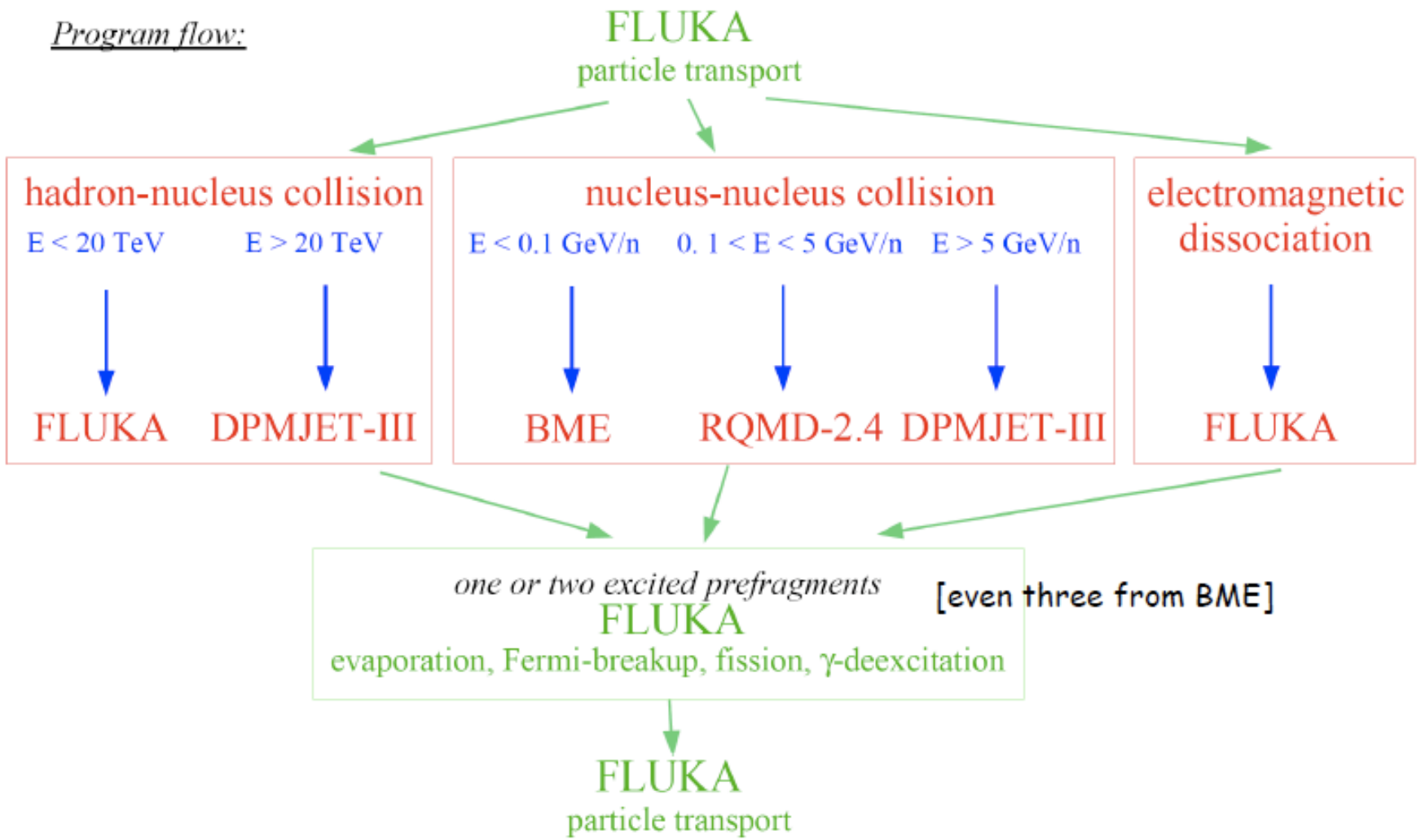

RQMD

E > 5 GeV/n

Dual Parton Model (DPM)
DPMJET-III (original code by R.Engel, J.Ranft and S.Roesler,
FLUKA-implemenation by T.Empl *et al.*)

0.1 GeV/n < E < 5 GeV/n

Relativistic Quantum Molecular Dynamics Model (RQMD)
RQMD-2.4 (original code by H.Sorge *et al.*,
FLUKA-implementation by A.Ferrari *et al.*)

E < 0.1 GeV/n

Boltzmann Master Equation (BME) theory
BME (original code by E.Gadioli et al.,
FLUKA-implementation by F.Cerutti et al.)

RQMD - *References*

interface to a suitably modified **RQMD model**

RQMD-2.4 (H. Sorge, 1998) was successfully applied

to relativistic A-A particle production over a wide energy range

[H. Sorge, Phys. Rev. **C 52**, 3291 (1995);

H. Sorge, H. Stöcker, and W. Greiner, Ann. Phys. **192**, 266 (1989)

and Nucl. Phys. **A 498**, 567c (1989)]

RQMD - *The original code*

The RQMD-2.4 code

INITIAL CONDITION two Fermi gases (projectile and target)

Fermi momentum $p_{F0} = \hbar \left(3\pi^2 \frac{A}{2V}\right)^{1/3}$ $V = (4/3)\,\pi \left(r_0 A^{1/3}\right)^3$ $r_0 = 1.12\,fm \Rightarrow \rho = 0.17\,\frac{nucl.}{fm^3}$

nucleon momentum $\boxed{p = p_{F0} \left(\frac{\rho(r)}{\rho_0}\right)^{\frac{1}{3}} \epsilon^{1/3}}$ $\epsilon \in [0, 1]$ random

$\phi = 2\pi\epsilon$ $\cos\theta = 1 - 2\epsilon$

$$p_x = p \sin\theta \cos\phi \quad - \left(\sum p_x\right)/A$$
$$p_y = p \sin\theta \sin\phi \quad - \left(\sum p_y\right)/A$$
$$p_z = p \cos\theta \quad - \left(\sum p_z\right)/A$$

so $\sum p_x = \sum p_y = \sum p_z = 0$

FINAL STATE

- $\left(p^0, p_x, p_y, p_z\right)$ for nucleons (and produced particles) in the LAB frame
- the spectators are marked
- no residue and fragment identification
- energy non-conservation issues, particularly when run in full QMD mode

RQMD - *The interfaced code*

Implemented developments

- construct the **projectile- and target-like** nuclei by gathering *spectator* nucleons,

assuming $E^{*}_{PL} = \sum_{pa,\ P} E_h \qquad (TL)$

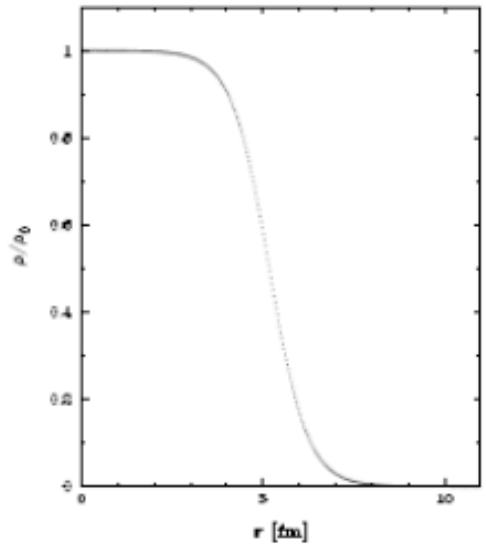

$$\rho(r) \propto \left(1 + \exp\left(\frac{r-R}{a}\right)\right)^{-1}$$

$$R = 1.19\,A^{1/3} - 1.61\,A^{-1/3}\ fm \qquad a = 0.52\ fm$$

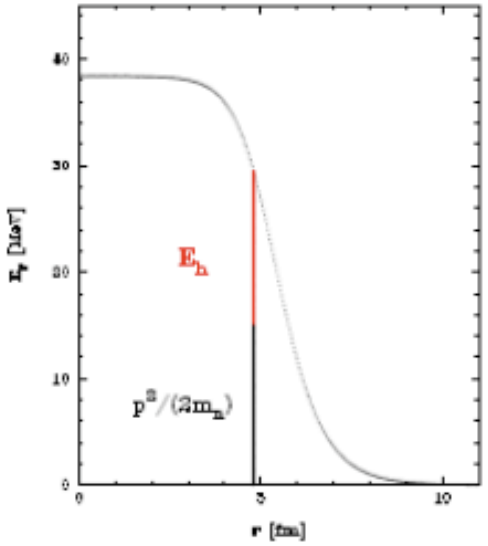

$$E_h = \frac{1}{2m_n}\left\{\left[p_{F0}\,(\rho(r)/\rho_0)^{1/3}\right]^2 - p^2\right\}$$

$$r, p\,(t=0)$$

- fix the remaining energy-momentum conservation issues taking into account **experimental binding energies**
- use the FLUKA evaporation/fission/fragmentation module

BME

E > 5 GeV/n

Dual Parton Model (DPM)
DPMJET-III (original code by R.Engel, J.Ranft and S.Roesler,
FLUKA-implemenation by T.Empl *et al.*)

0.1 GeV/n < E < 5 GeV/n

Relativistic Quantum Molecular Dynamics Model (RQMD)
RQMD-2.4 (original code by H.Sorge *et al.*,
FLUKA-implementation by A.Ferrari *et al.*)

E < 0.1 GeV/n

Boltzmann Master Equation (BME) theory
BME (original code by E.Gadioli *et al.*,
FLUKA-implementation by F.Cerutti *et al.*)

BME - *The interfaced code*

two different reaction paths have been adopted:

1. COMPLETE FUSION

$P_{CF}=\sigma_{CF}/\sigma_R$

pre-equilibrium

according to the BME theory

2. PERIPHERAL COLLISION

$P = 1 - P_{CF}$

work in progress

three body mechanism

pickup/stripping (for asymmetric systems at low *b*)

inelastic scattering (at high *b*)

FLUKA evaporation

1. In order to get the multiplicities of the pre-equilibrium particles and their double differential spectra, the BME theory is applied to a few representative systems at different bombarding energies and the results are parameterized.

2. The complete fusion cross section decreases with increasing bombarding energy. We integrate the nuclear densities of the projectile and the target over their overlapping region, as a function of the impact parameter, and obtain a preferentially excited "middle source" and two fragments (projectile- and target-like). The kinematics is suggested by break-up studies.

BME - *The database for the pre-equilibrium emissions*

^{16}O + ^{6}Li, ^{8}Li, ^{8}B, ^{10}B, ^{12}C, ^{14}N, ^{16}O, ^{19}F, ^{20}Ne, ^{24}Mg, ^{27}Al, ^{56}Fe, ^{197}Au

^{12}C + ^{8}Li, ^{8}B, ^{12}C, ^{27}Al, ^{40}Ca

@ 12, 30, 50, 70, 100 MeV/n

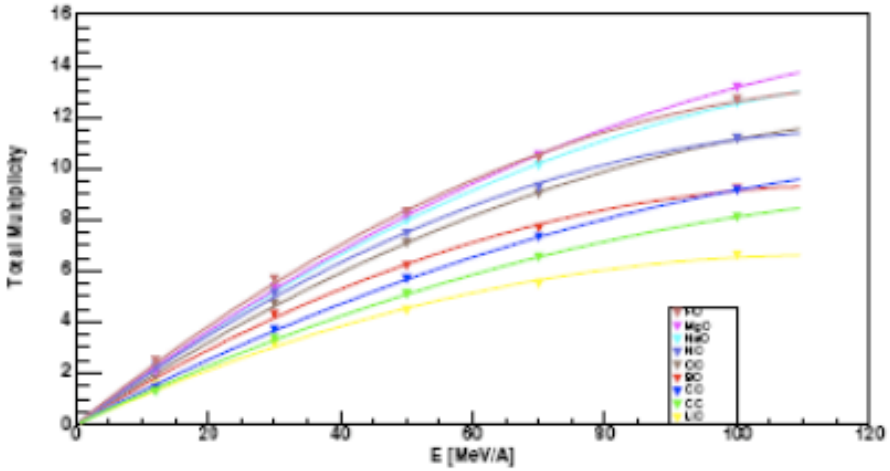

total multiplicity

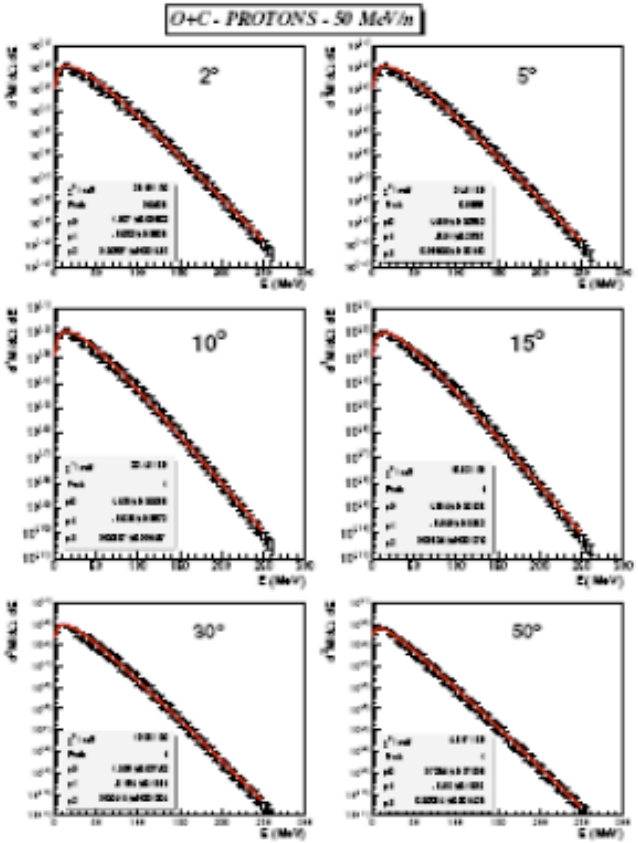

energy spectra

$$M = P_1 E_{nucl} - P_2 E_{nucl}^2$$

$$d^2M/(dEd\Omega) = E^{P_0(\theta)} \exp\left(-P_1(\theta) - P_2(\theta)E\right)$$

BME - *Theoretical framework*

Calculation of preequilibrium for the composite nucleus

proton and neutron momentum spaces divided into bins

$$\left\{(p_x, p_y, p_z) : p_z \in [p_{zi}, p_{zi} + \Delta p_z),\ \varepsilon = (2m)^{-1}\left(p_x^2 + p_y^2 + p_z^2\right) \in [\varepsilon_i, \varepsilon_i + \Delta\varepsilon)\right\}$$

(**z** is the beam direction)

of volume $2\pi m\,\Delta\varepsilon\,\Delta p_z$

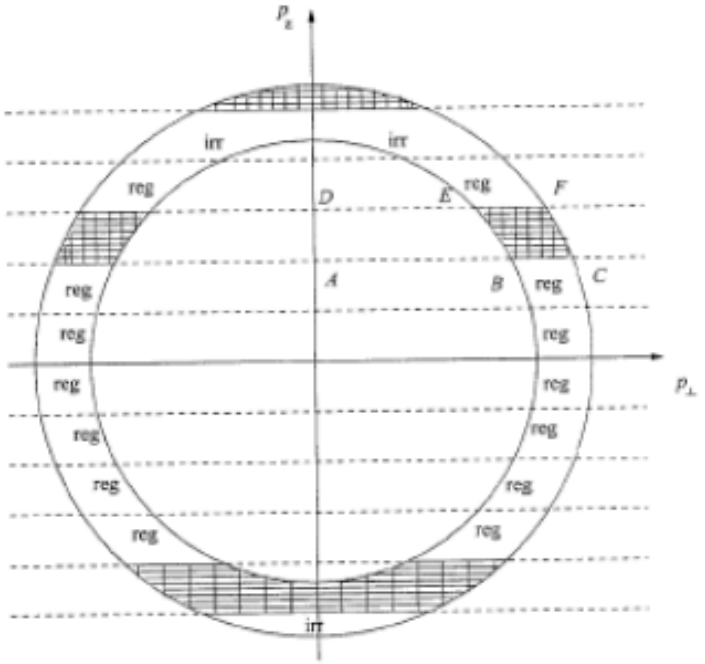

BME - *Theoretical framework*

The BME system

$N_i = n_i \; g_i$

- N_i: nucleon number
- n_i: occupation probability
- g_i: number of states in bin i

$$\frac{d(n_i^\pi g_i^\pi)}{dt} = \sum_{jlm} [\omega_{lm\to ij}^{\pi\pi} g_l^\pi n_l^\pi g_m^\pi n_m^\pi (1-n_i^\pi)(1-n_j^\pi) - \omega_{ij\to lm}^{\pi\pi} g_i^\pi n_i^\pi g_j^\pi n_j^\pi (1-n_l^\pi)(1-n_m^\pi)] + \sum_{jlm} [\omega_{lm\to ij}^{\pi\nu} g_l^\pi n_l^\pi g_m^\nu n_m^\nu (1-n_i^\pi)(1-n_j^\nu) - \omega_{ij\to lm}^{\pi\nu} g_i^\pi n_i^\pi g_j^\nu n_j^\nu (1-n_l^\pi)(1-n_m^\nu)] - n_i^\pi g_i^\pi \omega_{i\to i'}^\pi g_{i'}^\pi \delta(\varepsilon_i^\pi - \varepsilon_{i'}^\pi - \varepsilon_F^\pi - B^\pi) - \frac{dD_i^\pi}{dt}$$

BME - *Theoretical framework*

Multiplicity spectra

of emitted nucleons

$$\frac{d^2M(\varepsilon',\theta)}{d\varepsilon'\,d\Omega} = \frac{1}{2\pi\sin\theta}\int_0^{t_{eq}} n(\varepsilon,\theta,t)\,\frac{\sigma_{inv}\,V}{V}\,\rho(\varepsilon',\theta)\,dt$$

of a cluster c

$$\frac{d^2M_c(E_c',\theta_c)}{dE_c'\,d\Omega} = \frac{R_c}{2\pi\sin\theta}\int_0^{t_{eq}} N_c(E_c,\theta_c,t)\,\frac{\sigma_{inv,c}\,V_c}{V}\,\rho_c(E_c',\theta_c)\,dt$$

$$N_c(E_c,\theta_c,t) = \prod_i \left(n_i^{\pi}(\varepsilon,\theta,t)\right)^{P_i(E_c,\theta_c)Z_c} \cdot \prod_i \left(n_i^{\nu}(\varepsilon,\theta,t)\right)^{P_i(E_c,\theta_c)N_c}$$

joint probability

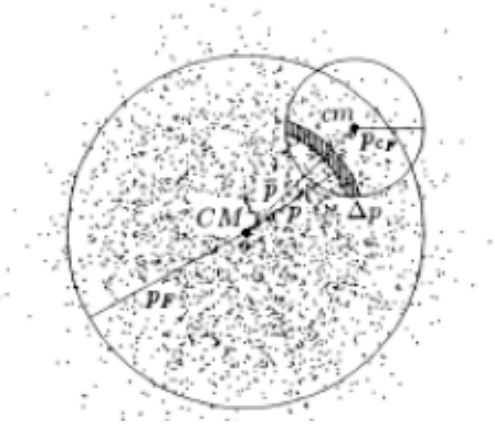

BME - *Peripheral collisions*

i. selection of the *impact parameter b*

ii. kinematics determination

θ_{PL} , θ_{TL} chosen according to $[d\sigma/d\Omega]_{cm} \sim \exp(-k\theta_{cm})$
θ_{MS} momentum conservation
p_{PL} , p_{TL} chosen according to a given energy loss distribution
p_{MS} momentum conservation
ϕ_{PL} free
ϕ_{TL} , ϕ_{MS} same reaction plane

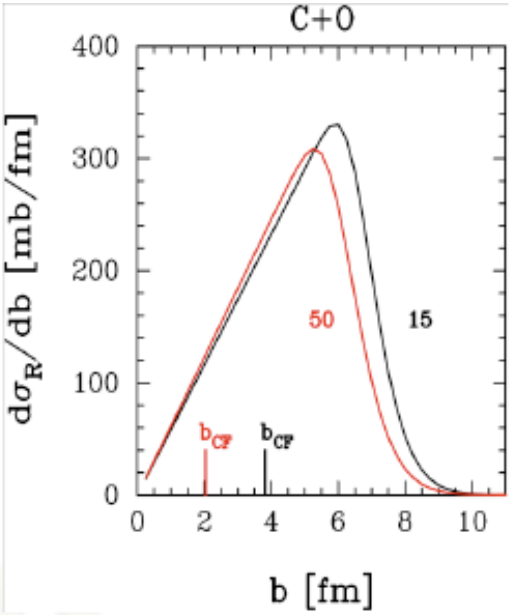

work in progress

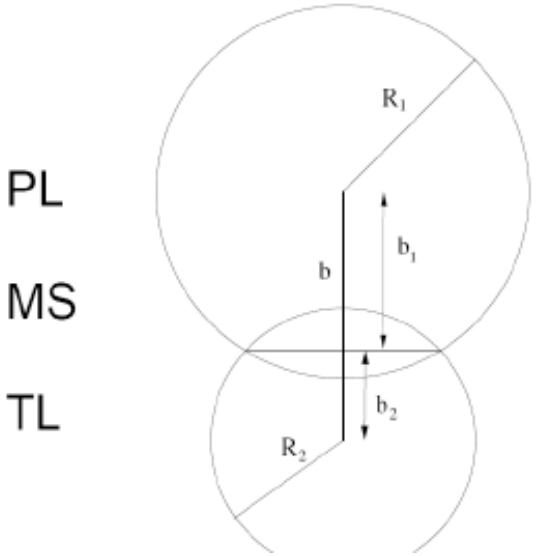

iii. excitation energy sharing

$$E^{\star}_{MS} = (A_{MS}/A_{tot})E^{\star}_{tot}\sum_{n=0}^{k}(1 - A_{MS}/A_{tot})^{n}$$

$$E^{\star}_{PL} = f(A_{PL}, A_{TL})\left(E^{\star}_{tot} - E^{\star}_{MS}\right)$$

$$E^{\star}_{TL} = \left(E^{\star}_{tot} - E^{\star}_{MS} - E^{\star}_{PL}\right)$$

The FLUKA Monte Carlo code

- Reliable Nuclear Models
- Already applied to proton therapy:

  - Dosimetric/radiobiological studies (Biaggi *et al* NIM B 159, 1999)

- Import of raw CT scans with optimized algorithms for efficient transport in voxel geometries (Andersen *et a*l Rad. Prot. Dos. 116, 2005)
- Huge efforts for ion transport in connection with NASA grant (2000)
- Very promising results from initial studies of ion beam fragmentation in water (Sommerer *et al* PMB 51, 2006, A. Mairani PhD Thesis 2007, Pavia)

Mixed Radiation Field in Carbon Ion Therapy

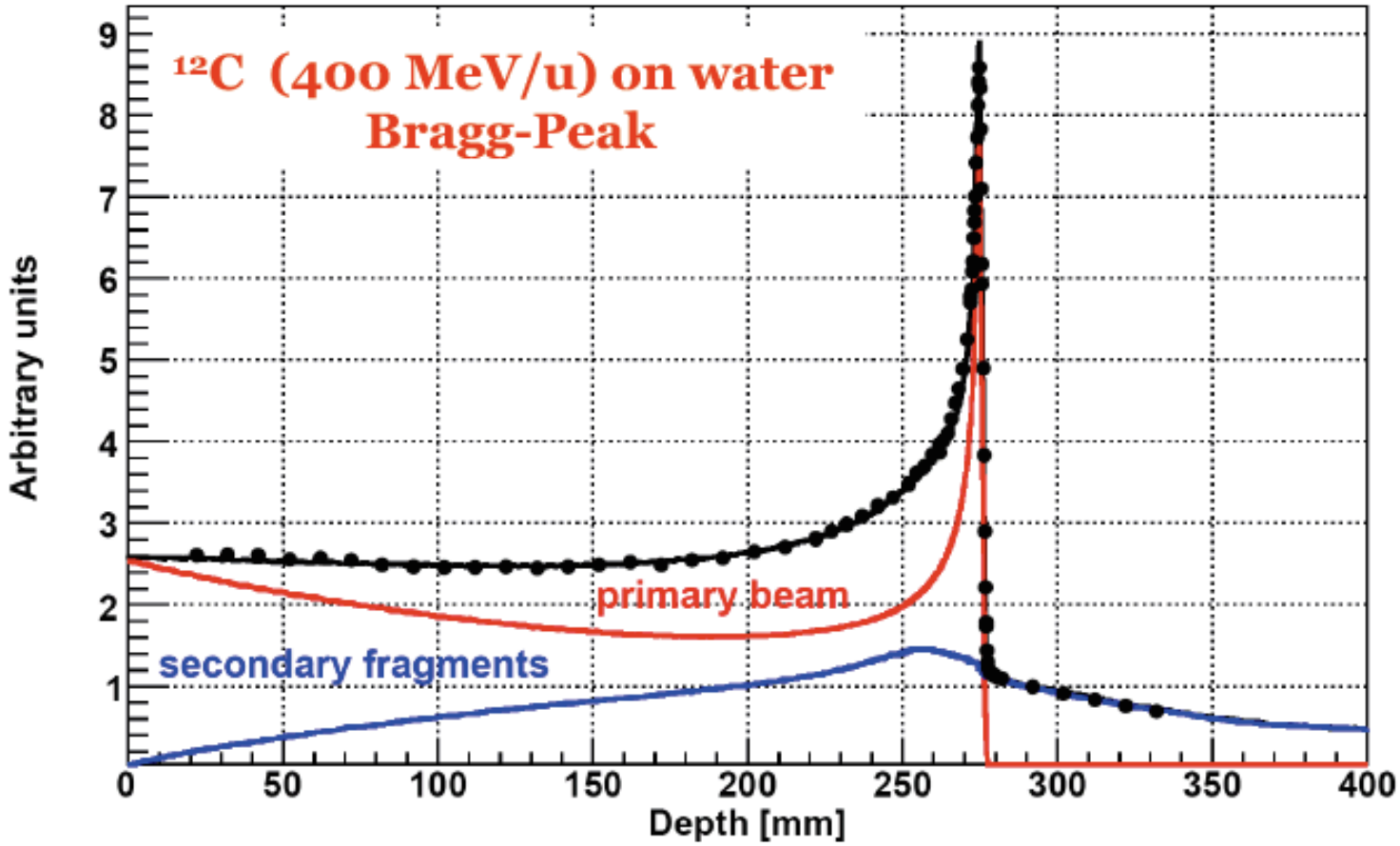

Exp. Data (points) from Haettner et al, Rad. Prot. Dos. 2006

Simulation: A. Mairani PhD Thesis, 2007, Nuovo Cimento C, 31, 2008

Lateral scattering

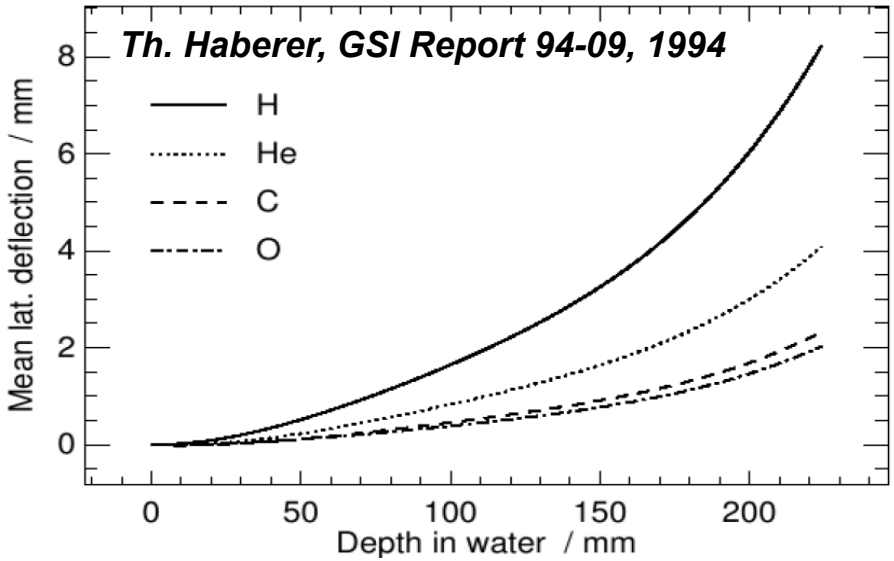

Ions heavier than protons have a reduced lateral scattering

Monitoring with PET

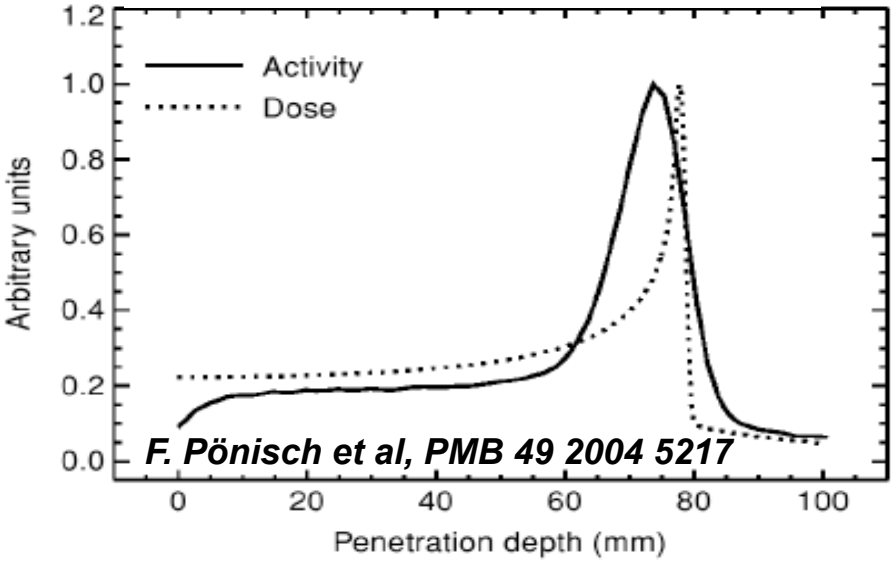

Mixed Radiation Field in Carbon Ion Therapy

^{12}C (400 MeV/u) on water

Attenuation of primary beam

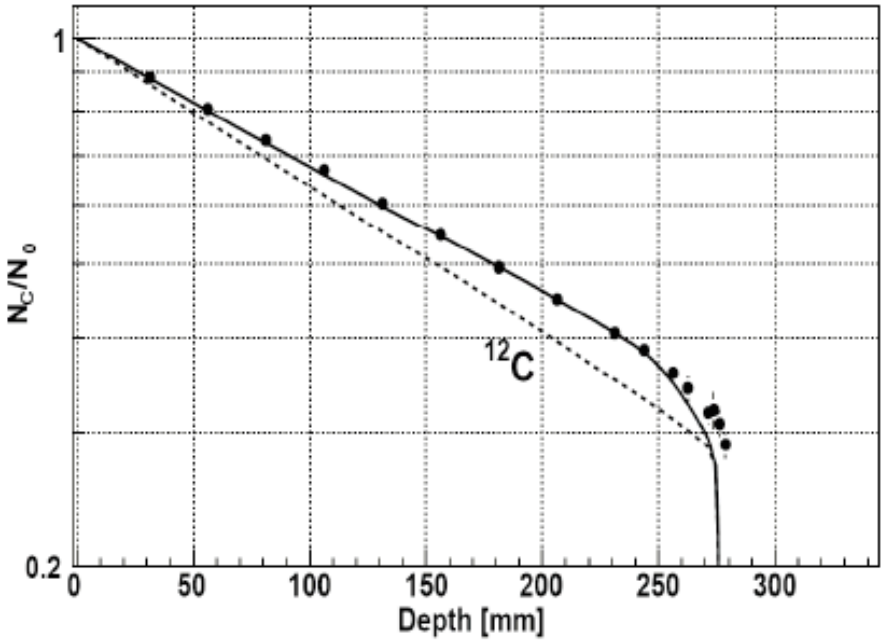

Build-up of secondary fragments

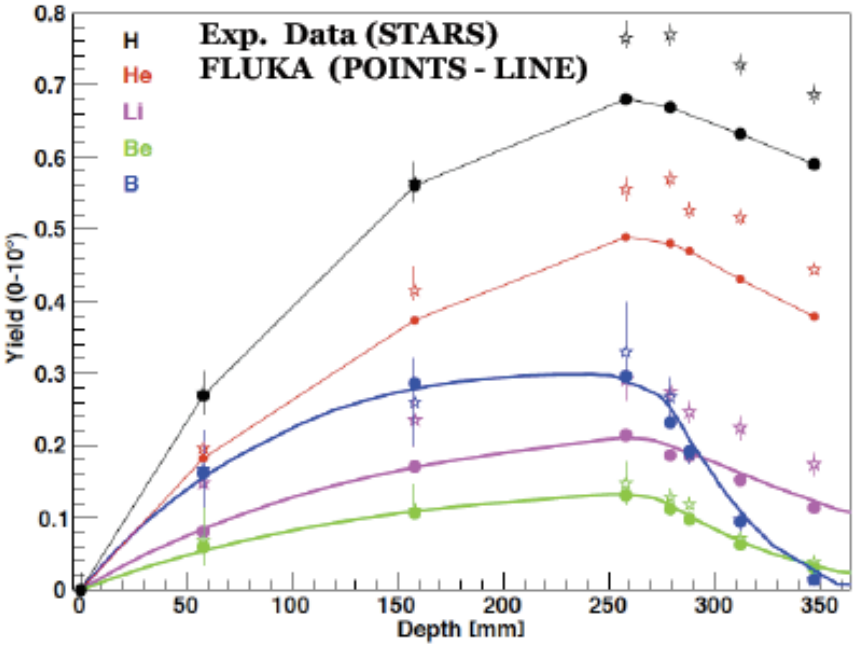

Exp. Data (points) from Haettner et al, Rad. Prot. Dos. 2006

Simulation: A. Mairani PhD Thesis, 2007, PMB *to be published*

Mixed Radiation Field in Carbon Ion Therapy

^{12}C (400 MeV/u) on water

Angular distribution

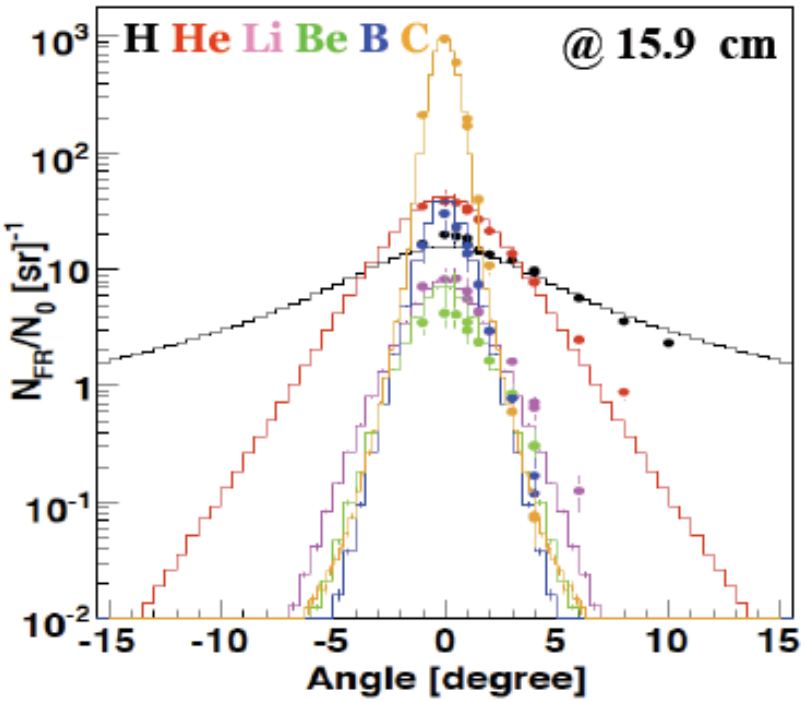

Energy distribution

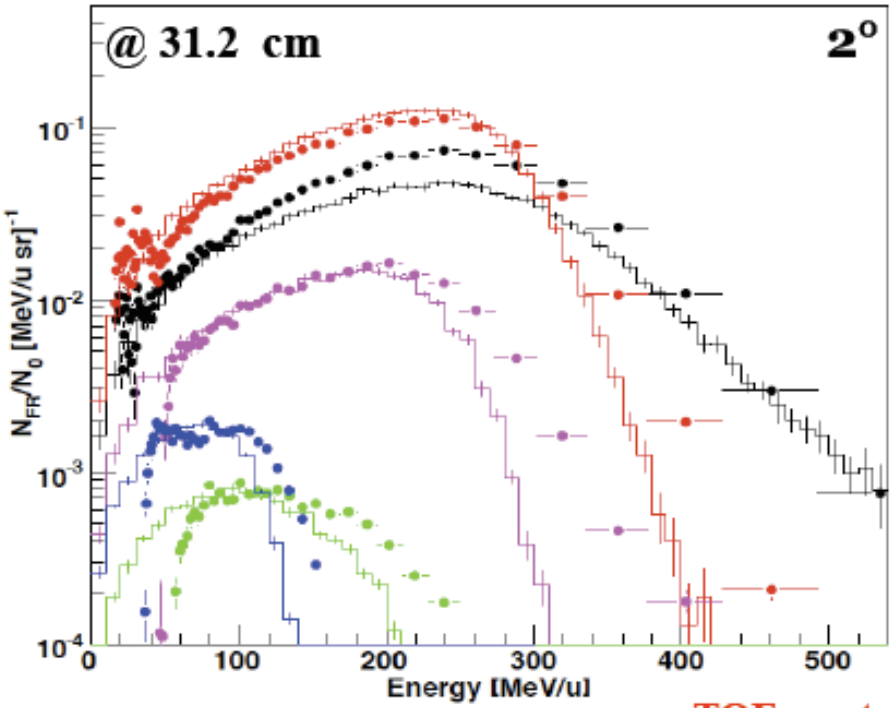

TOF spectra in progress

Exp. Data (points) from Haettner et al, Rad. Prot. Dos. 2006

Simulation: A. Mairani PhD Thesis, 2007, PMB *to be published*

The commonly recognized merits of MC

MC are powerful computational tools for:

- Realistic description of particle interactions, especially in complex geometries and inhomogeneous media where analytical approaches are at their limits of validity
- Possibility to investigate separate contributions to quantities of interest which may be impossible to be experimentally assessed and/or discriminated

The commonly recognized merits of MC

MC are powerful computational tools for:

- Realistic description of particle interactions, especially in complex geometries and inhomogeneous media where analytical approaches are at their limits of validity
- Possibility to investigate separate contributions to quantities of interest which may be impossible to be experimentally assessed and/or discriminated

The role of MC in ion therapy

Treatment planning systems (TPS) use analytical models

MC are increasingly used tools to support:

- ***Startup and Commissioning of new facilities:*** e.g., shielding calculations; beamline modeling, generation of TPS input data (↓ *meas. time*)
- ***Validation of TPS dose calculations:*** in water-equivalent system and in patient anatomy (CT)
- ***Dedicated applications:*** imaging of secondary emerging radiation for treatment verification (PET, prompt gamma…)

Simulation packages used in ion therapy

General-purpose condensed-history MC codes

- FLUKA *(www.fluka.org)*
- Geant4 *(www.cern.ch/geant4)*
- MCNPX *(mcnpx.lanl.gov)*
- PHITS *(phits.jaea.go.jp)*

… and others…

Capable to handle all ion beams of therapeutic relevance

Dedicated MC codes for proton dose calculations

VMCpro, Fippel and Sokoup, MP 31, 2004

PSI, A Tourovsky et al, PMB 50,2005

Different ion beam delivery strategies

Passive conformation of scattered broad beam with compensator (distal edge) and collimator (lateral shaping)

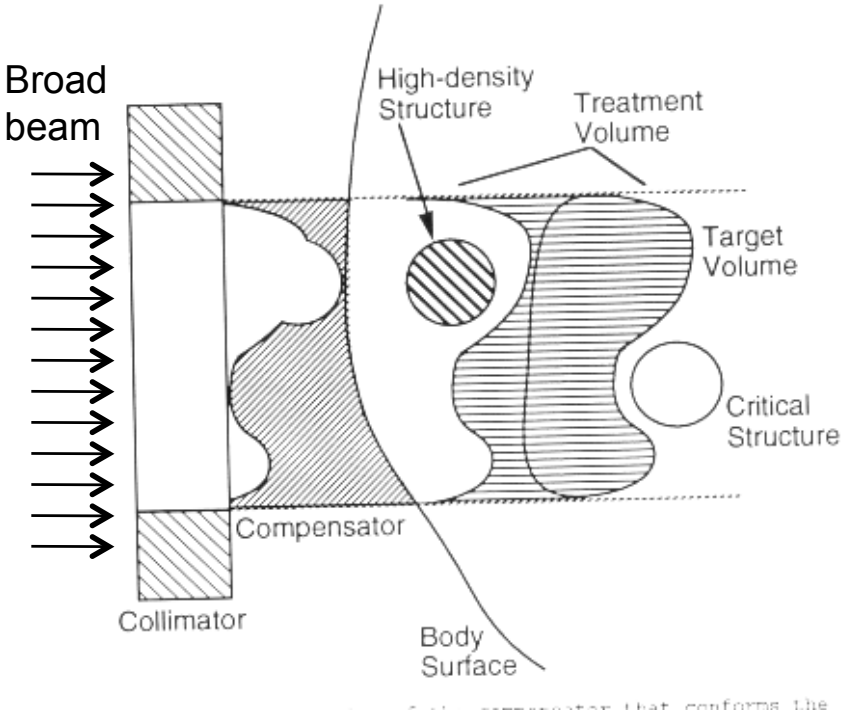

Chu et al, Rev Sci Instrum 1993

Active conformation via energy variation and lateral magnetic deflection of pencil-like beams

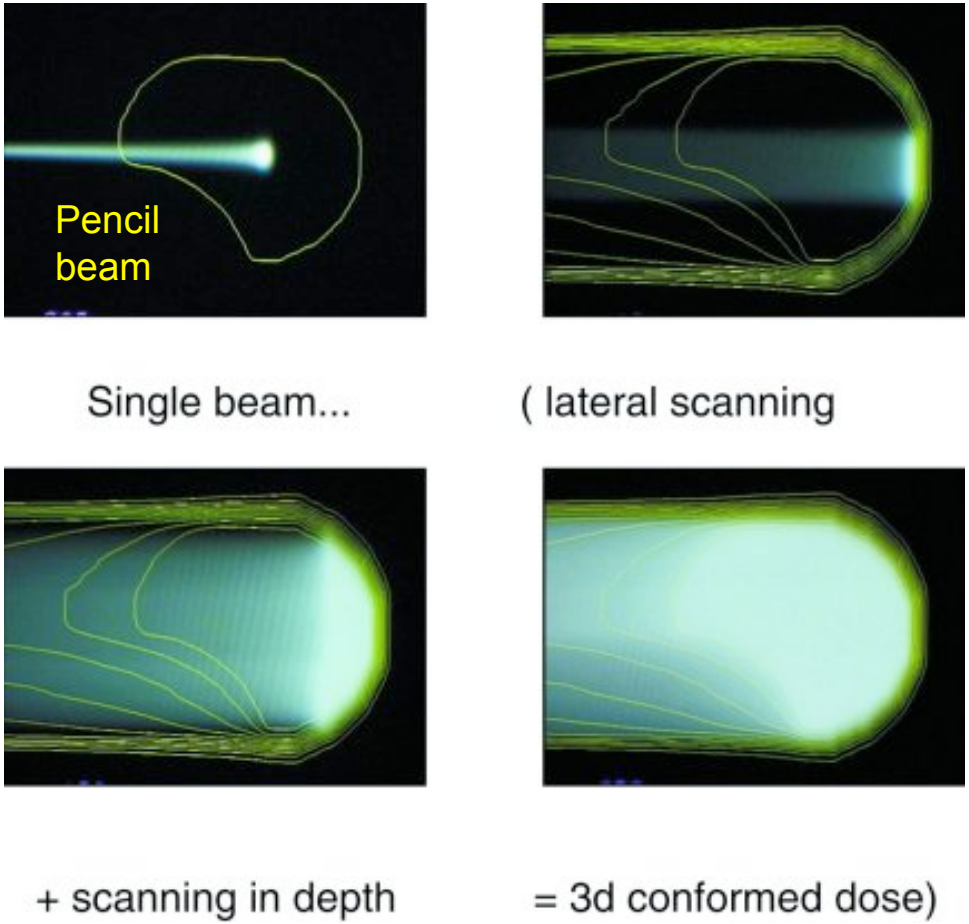

http://p-therapie.web.psi.ch/

MC application to passive beam delivery

Geant4-based modeling of nozzle at MGH Proton Center

- MC model of the nozzle components with mm-accuracy (~1000 objects)
- MC settings (e.g., initial beam energy, spread and size) based on available information (measured or from manufacturer) or tuned on exp. data

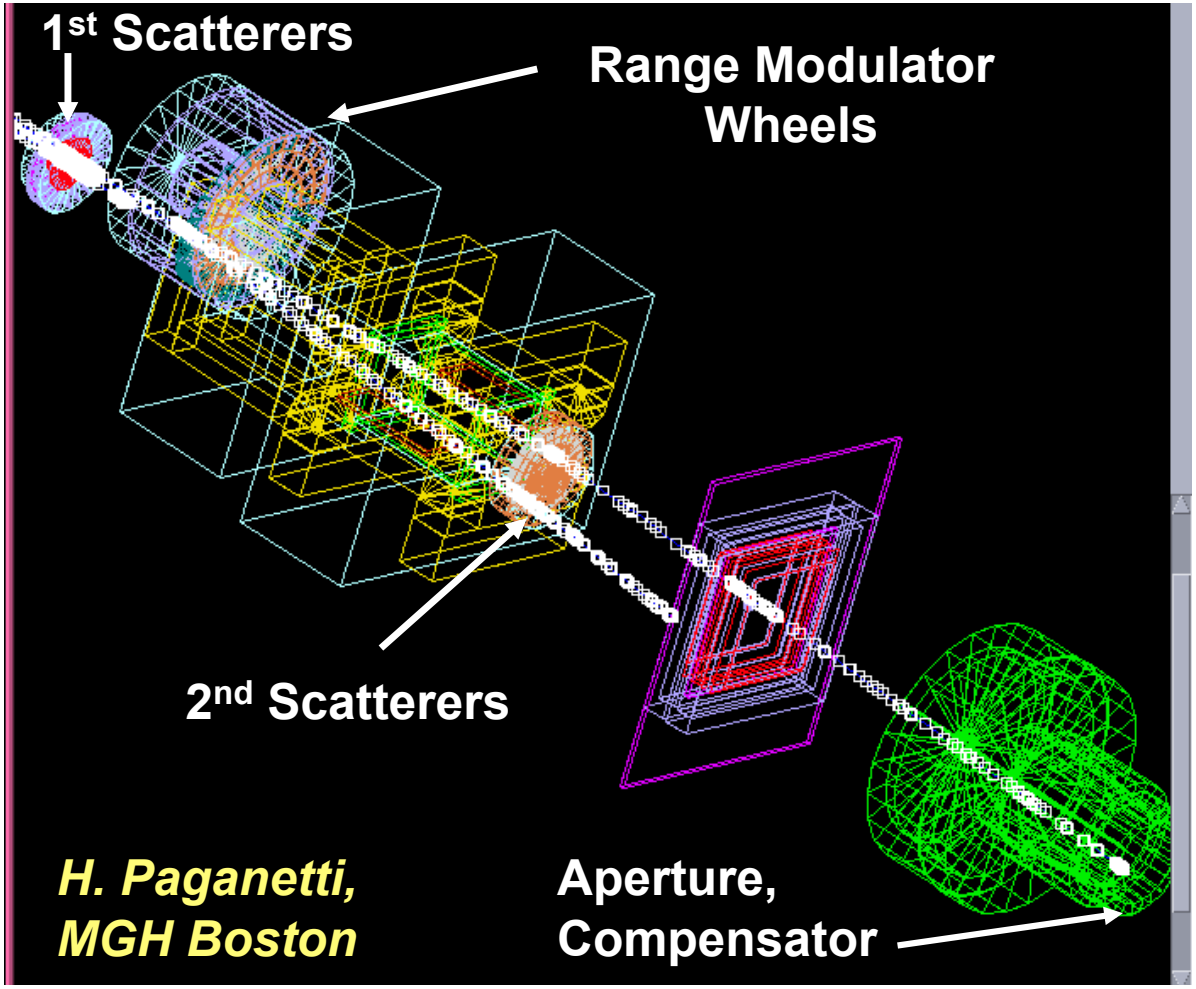

Paganetti et al, Med. Phys. 2004

MC application to active beam delivery @ HIT

Ion species

- *p*, ^{12}C
  (later also ^{3}He, ^{16}O)

Beam delivery

- Scanning with active energy variation (like @ GSI)
- Required parameters:

255 Energy steps
4 Foci
10 Intensities

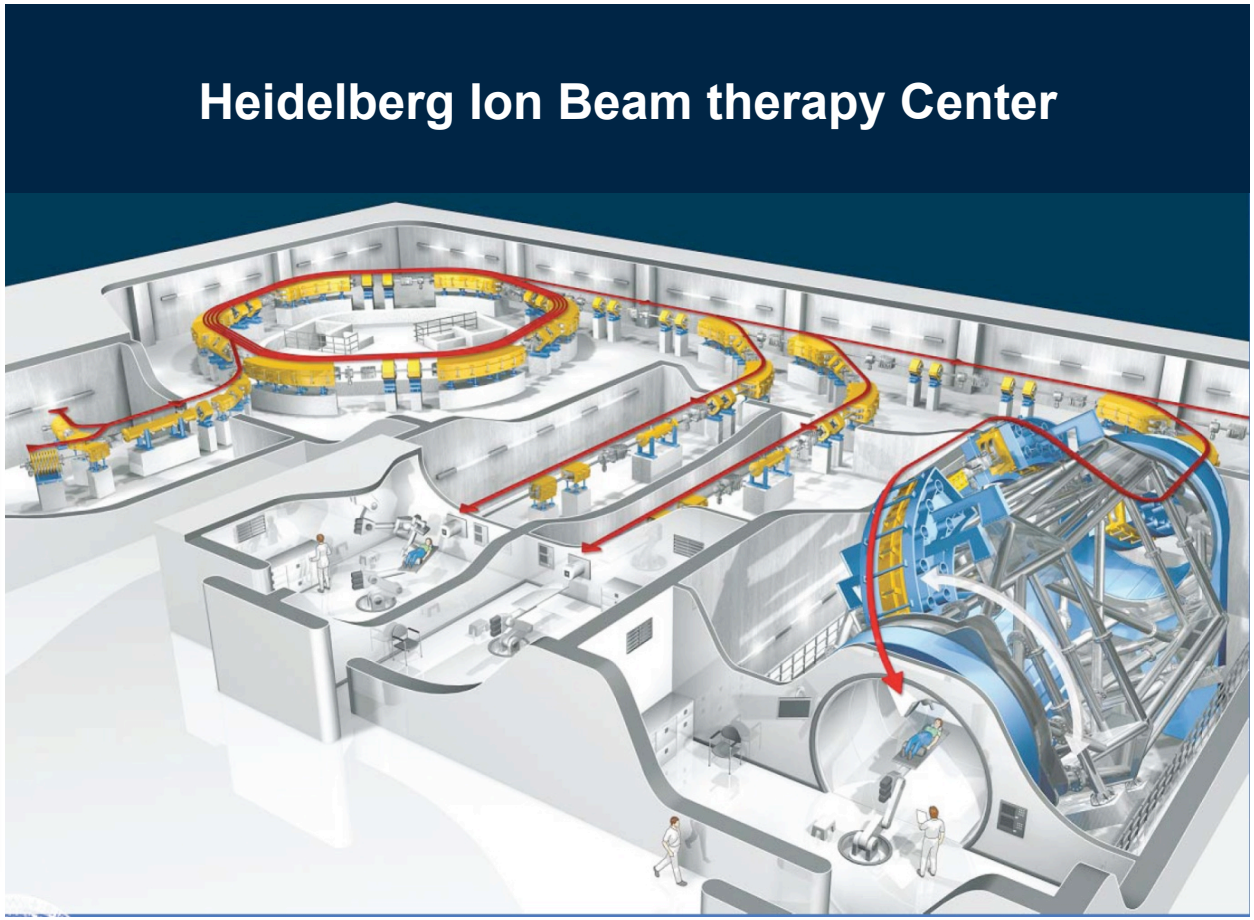

MC application to active beam delivery @ HIT

Ion species

- *p*, ^{12}C
  (later also ^{3}He, ^{16}O)

Beam delivery

- Scanning with active energy variation (like @ GSI)
- Required parameters:
  255 Energy steps
  4 Foci
  10 Intensities

MC (FLUKA) simulations

Parodi, Brons, Naumann, Haberer et al, to be published

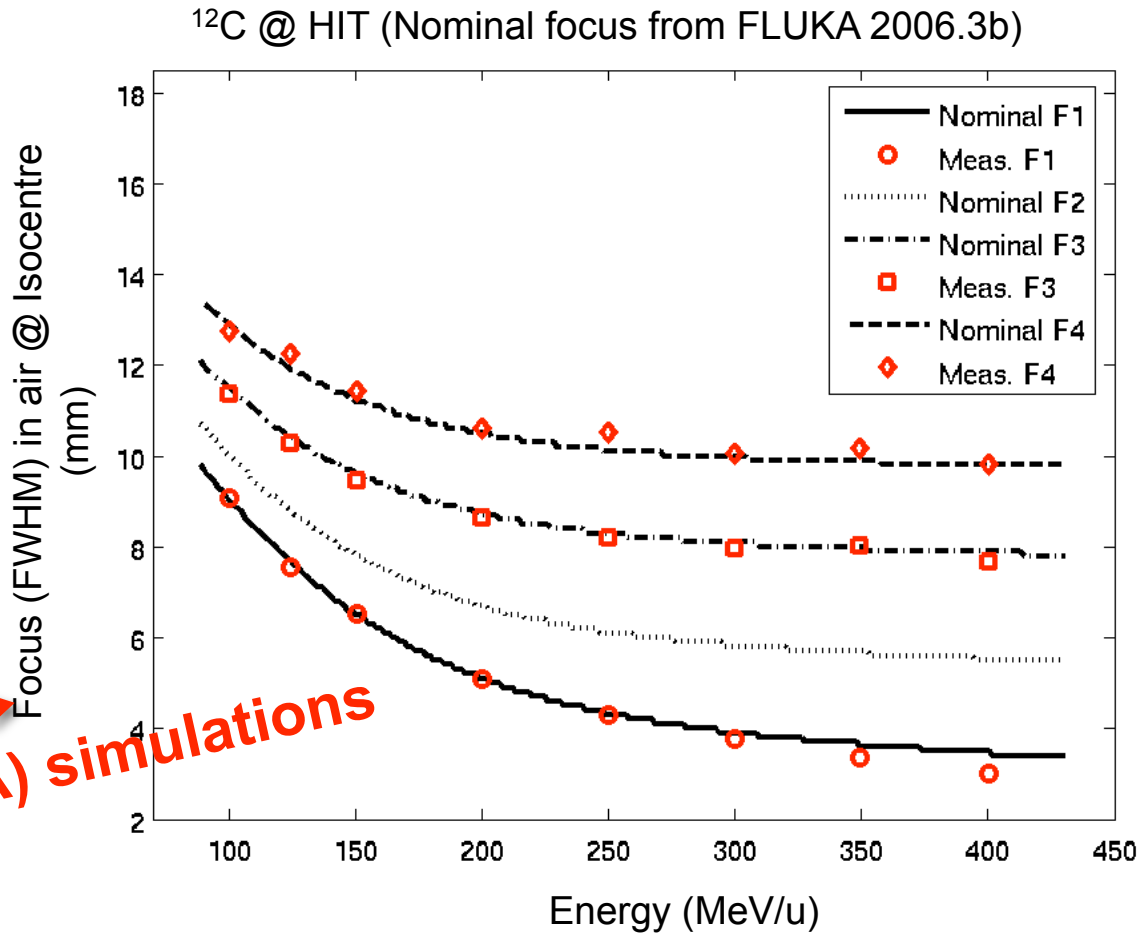

…Taking into account desired 4-10 mm focus @ ISO for higher E and physical limitation from scattering in monitor system and air

MC application to active beam delivery @ HIT

MC forward recalculation of TPS treatment plans in water
(i.e. medium where plans are experimentally verified)
FLUKA coupled with control file of raster scanning system

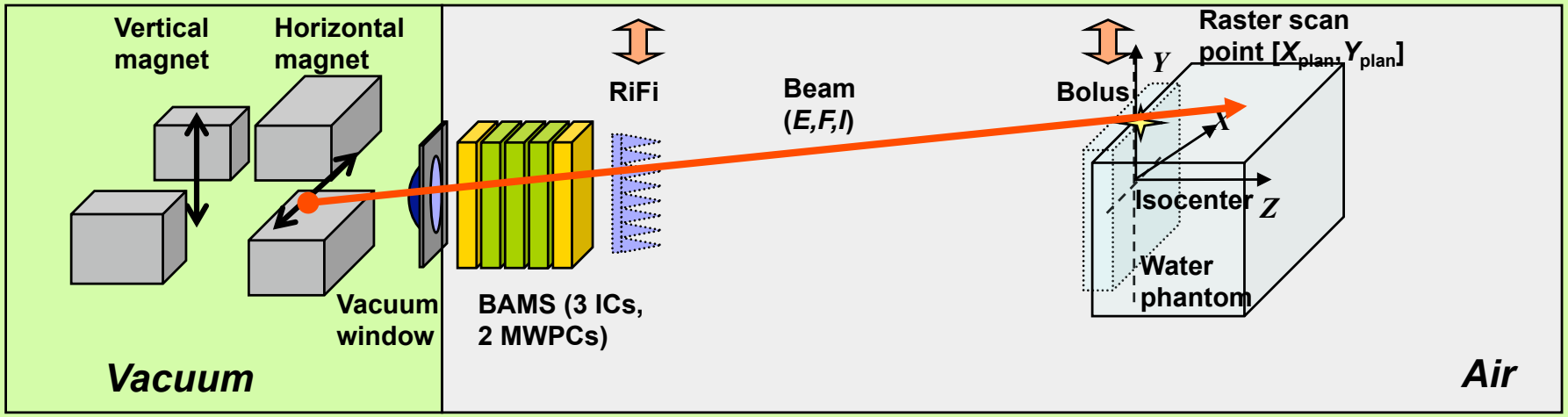

(F. Sommerer et al, EWG-MCTP Workshop, Ghent 2006; Parodi, Mairani, Sommerer et al, to be published)

Experimental validation of the MC

MC calculation of scanned carbon ion SOBP at HIT
(A. Mairani et al, to be published)

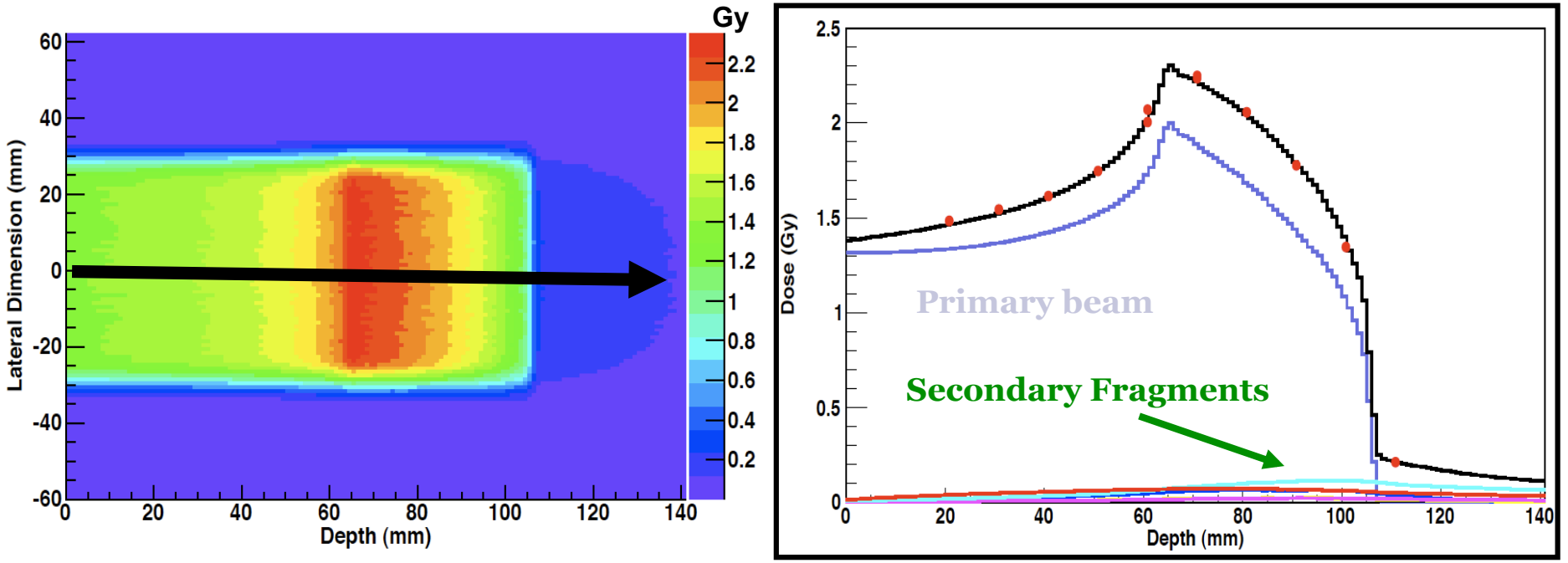

Exp. IC measurements in water (points) courtesy of M. Winter and S. Brons (HIT)

From dose in water to dose in patient CT

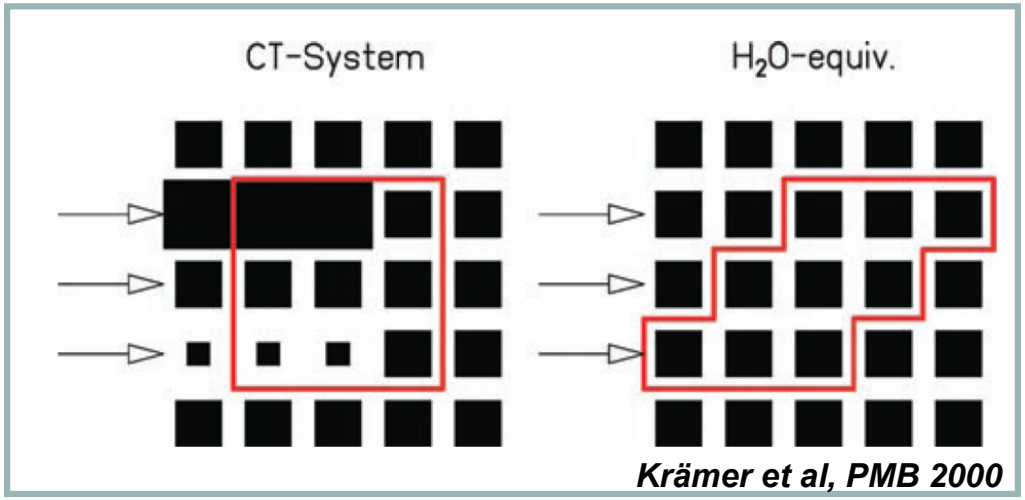

Krämer et al, PMB 2000

The typical TPS approach

Scale dose-to-water according to radiological path length deduced from semi-empirical CT-range calibration curve

CT Number = Hounsfield Unit

HU = 1000 (μ_x-μ_{H_2O}) / μ_{H_2O}

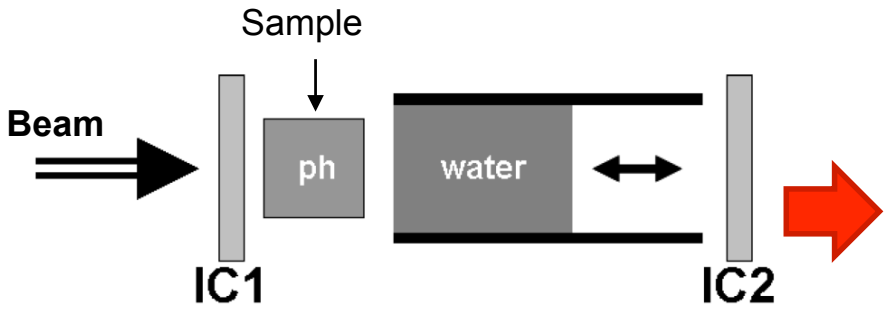

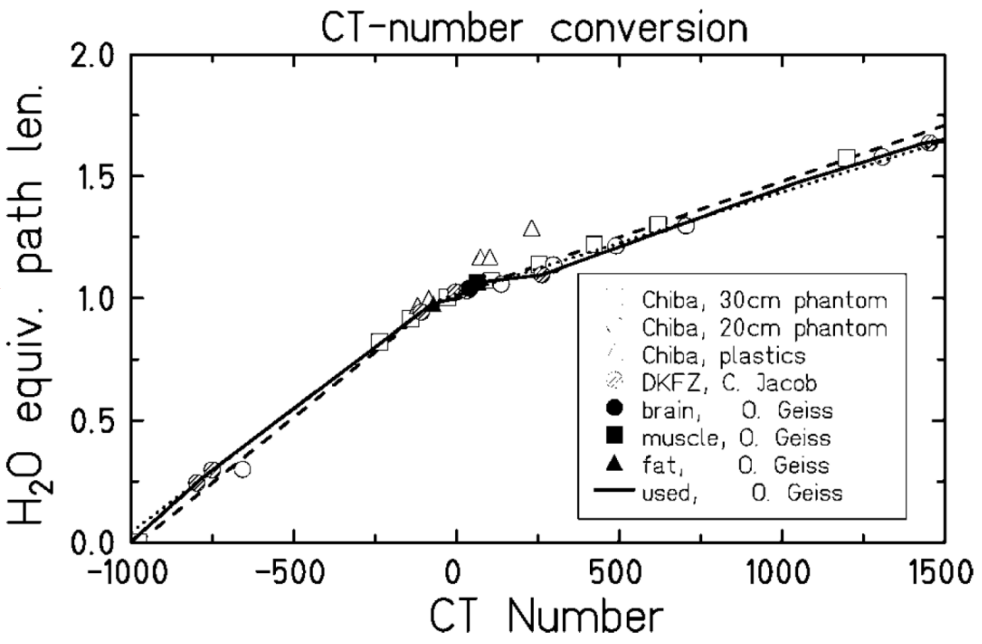

Rietzel et al, Radiat Oncol 2008

Krämer et al, PMB 2000

MC CT-based dose calculations @ MGH / GSI /HIT

- CT segmentation into **27 materials** of defined elemental composition
  (24 taken from Schneider et al 2000, extended in Parodi et al 2007 up to HU ≥ 3060 for Ti)
- "Nominal" mean density given to each material *(Jiang et al MP 31, 2004, Parodi et al PMB 2007, Paganetti et al PMB 2009)*
- HU-dependent correction factors accounting for "real density" dependence and HU-range calibration curve as TPS ($dEdx_{HU} / dEdx_{H2O}$)

HU	w_i (pp)											
	H	C	N	O	Na	Mg	P	S	Cl	Ar	K	Ca
−1000–−950			75.5	23.2						1.3		
−950–−120	10.3	10.5	3.1	74.9	0.2		0.2	0.3	0.3		0.2	
−120–−83	11.6	68.1	0.2	19.8	0.1			0.1	0.1			
−82–−53	11.3	56.7	0.9	30.8	0.1			0.1	0.1			
−52–−23	11.0	45.8	1.5	41.1	0.1		0.1	0.2	0.2			
−22–7	10.8	35.6	2.2	50.9			0.1	0.2	0.2			
8–18	10.6	28.4	2.6	57.8			0.1	0.2	0.2		0.1	
19–80	10.3	13.4	3.0	72.3	0.2		0.2	0.2	0.2		0.2	
80–120	9.4	20.7	6.2	62.2	0.6			0.6	0.3			
120–200	9.5	45.5	2.5	35.5	0.1		2.1	0.1	0.1		0.1	4.5
200–300	8.9	42.3	2.7	36.3	0.1		3.0	0.1	0.1		0.1	6.4
300–400	8.2	39.1	2.9	37.2	0.1		3.9	0.1	0.1		0.1	8.3
400–500	7.6	36.1	3.0	38.0	0.1	0.1	4.7	0.2	0.1			10.1
500–600	7.1	33.5	3.2	38.7	0.1	0.1	5.4	0.2				11.7
600–700	6.6	31.0	3.3	39.4	0.1	0.1	6.1	0.2				13.2
700–800	6.1	28.7	3.5	40.0	0.1	0.1	6.7	0.2				14.6
800–900	5.6	26.5	3.6	40.5	0.1	0.2	7.3	0.3				15.9
900–1000	5.2	24.6	3.7	41.1	0.1	0.2	7.8	0.3				17.0
1000–1100	4.9	22.7	3.8	41.6	0.1	0.2	8.3	0.3				18.1
1100–1200	4.5	21.0	3.9	42.0	0.1	0.2	8.8	0.3				19.2
1200–1300	4.2	19.4	4.0	42.5	0.1	0.2	9.2	0.3				20.1
1300–1400	3.9	17.9	4.1	42.9	0.1	0.2	9.6	0.3				21.0
1400–1500	3.6	16.5	4.2	43.2	0.1	0.2	10.0	0.3				21.9
1500–1600	3.4	15.5	4.2	43.5	0.1	0.2	10.3	0.3				22.5

Schneider et al PMB 45, 2000 (based on analysis of 71

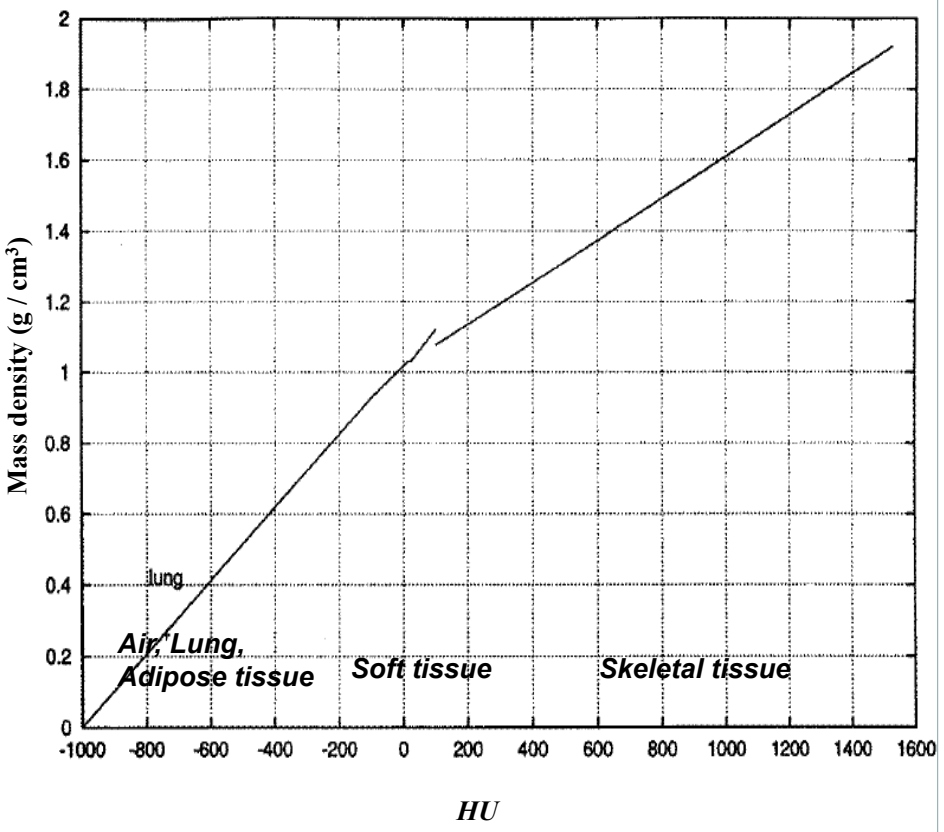

MC versus TPS dose for passive delivery @ MGH

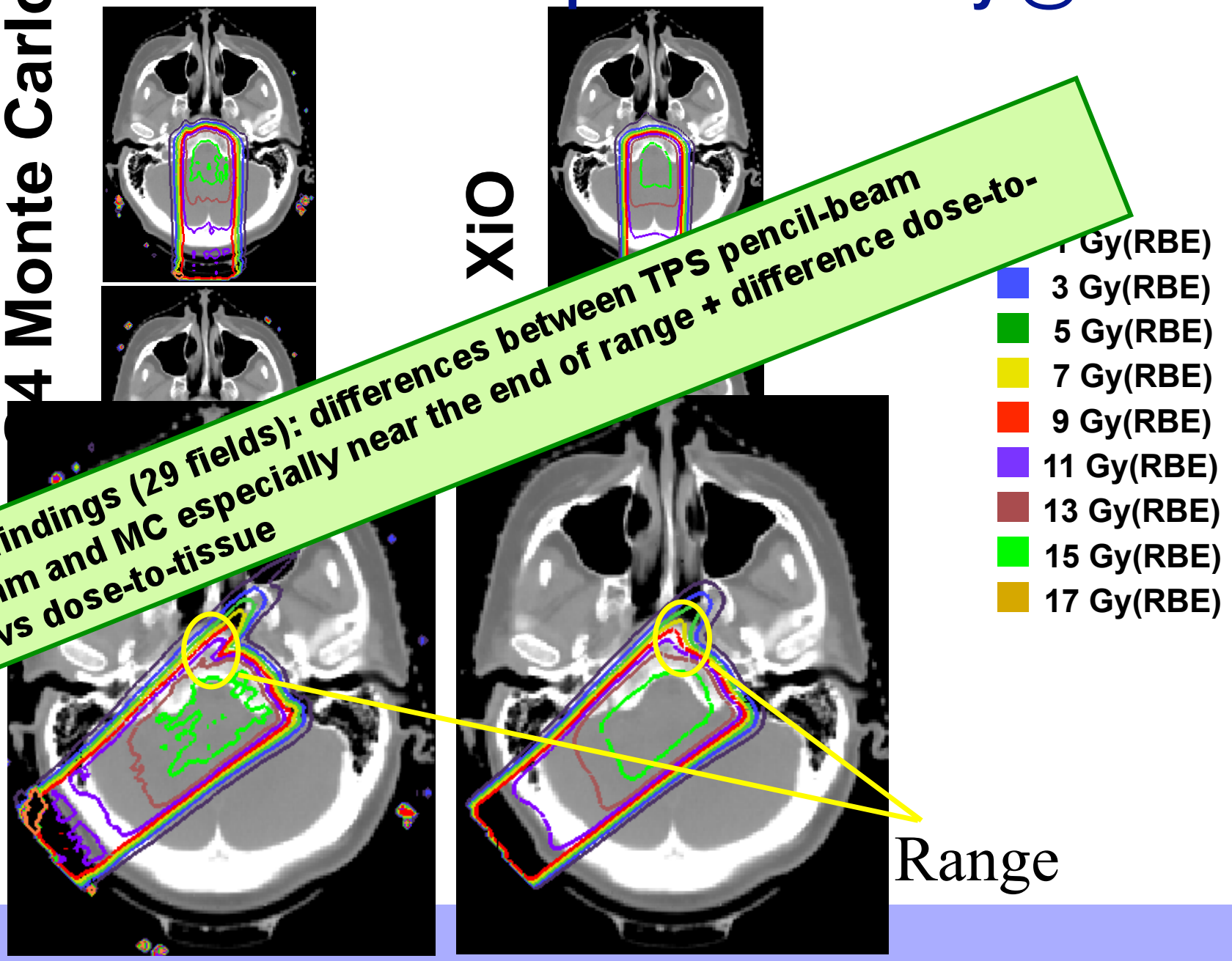

Paganetti et al, Phys. Med. Biol. 53, 2008

MC versus TPS for proton therapy @ MGH

Paraspinal tumor patient with metallic implants

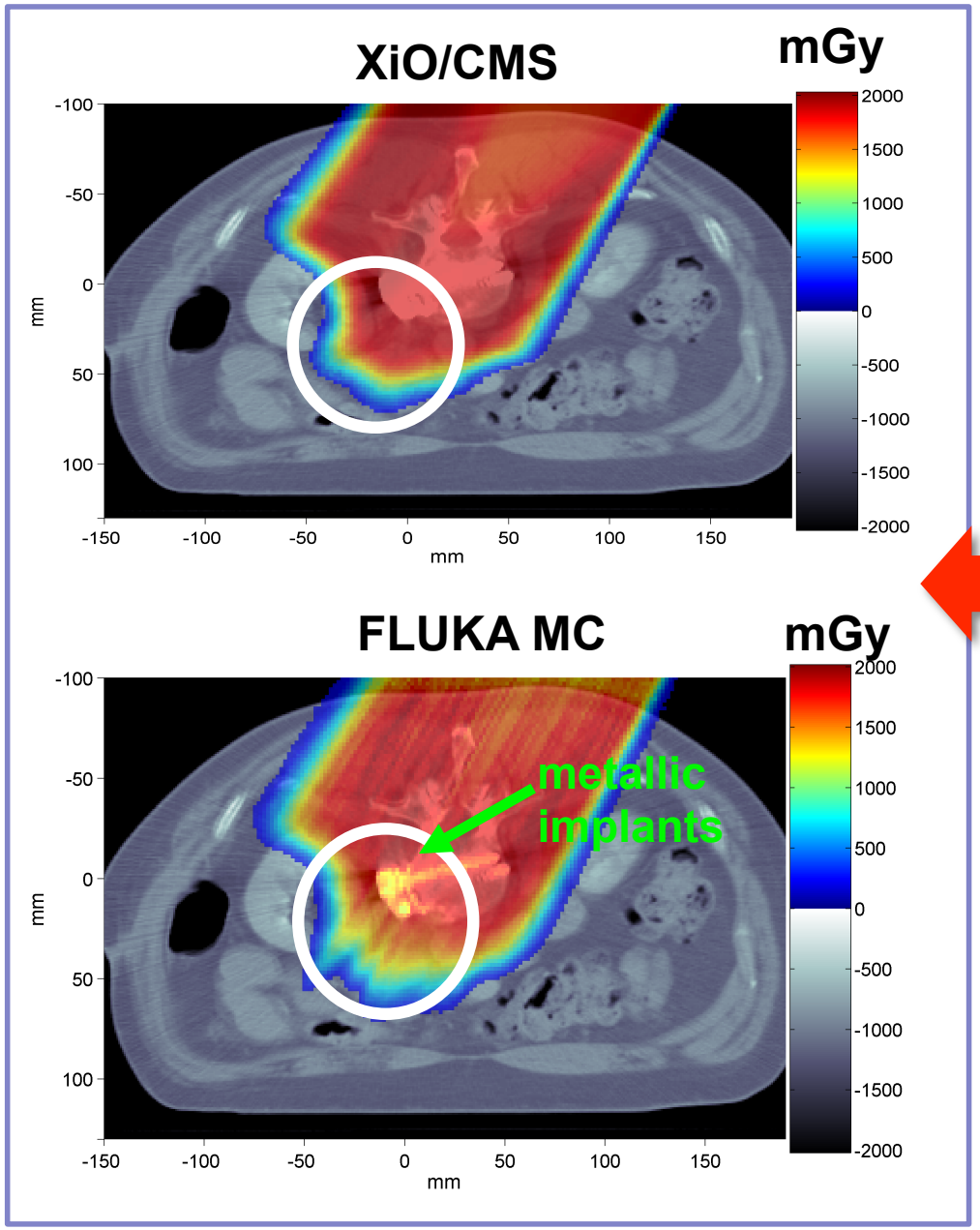

Useful tools to validate critical TPS plans, e.g., with large tissue inhomogeneities, **metallic implants**

Prescribed proton dose: 1.8 Gy
MC : ~ 7.4 10^7 *p* in 12 runs

Parodi et al, IJROBP 2007

MC versus TPS dose for scanned ^{12}C @ GSI/HIT

Inhomogeneities, dose-to-tissue and dose-to water, fragmentation tail

Prescribed dose ~ 0.25 Gy
MC ~ 1.7 10^7 ^{12}C in 10 runs

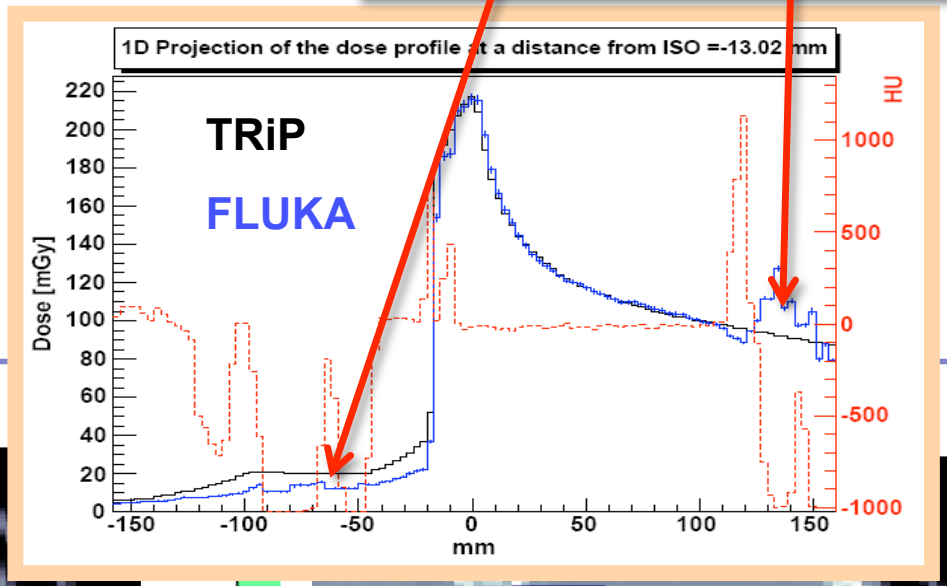

Clivus Chordoma Patient

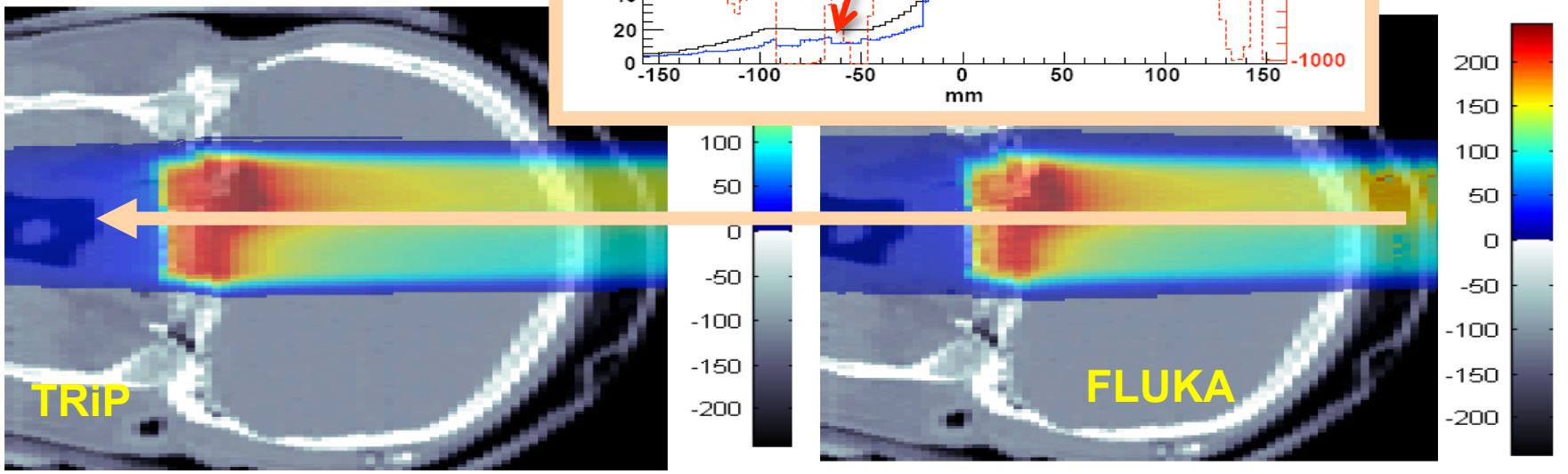

Mairani, Ph.D. Thesis; Mairani, Parodi et al, IEEE CR 2008

Dose-to-water versus Dose-to-tissue

Analytical dose calculation algorithms results in dose-to-water
(because materials are characterized by relative stopping powers)

Monte Carlo results in dose-to-tissue
(because materials are characterized by material compositions, mass densities, ionization potentials)

- H. Paganetti recently proposed a formalism to convert MC calculated dose-to-tissue into dose-to-water in proton therapy ***(Phys. Med. Biol. 54, 2009)***
- Three approaches of increasing accuracy were studied, based on

1. *Average stopping power ratios*
2. *Energy-dependent stopping power ratios*
3. *Energy-dependent stopping power ratios and nuclear interactions*

Dose-to-water versus Dose-to-tissue

Patient 1: spinal meninges chordoma

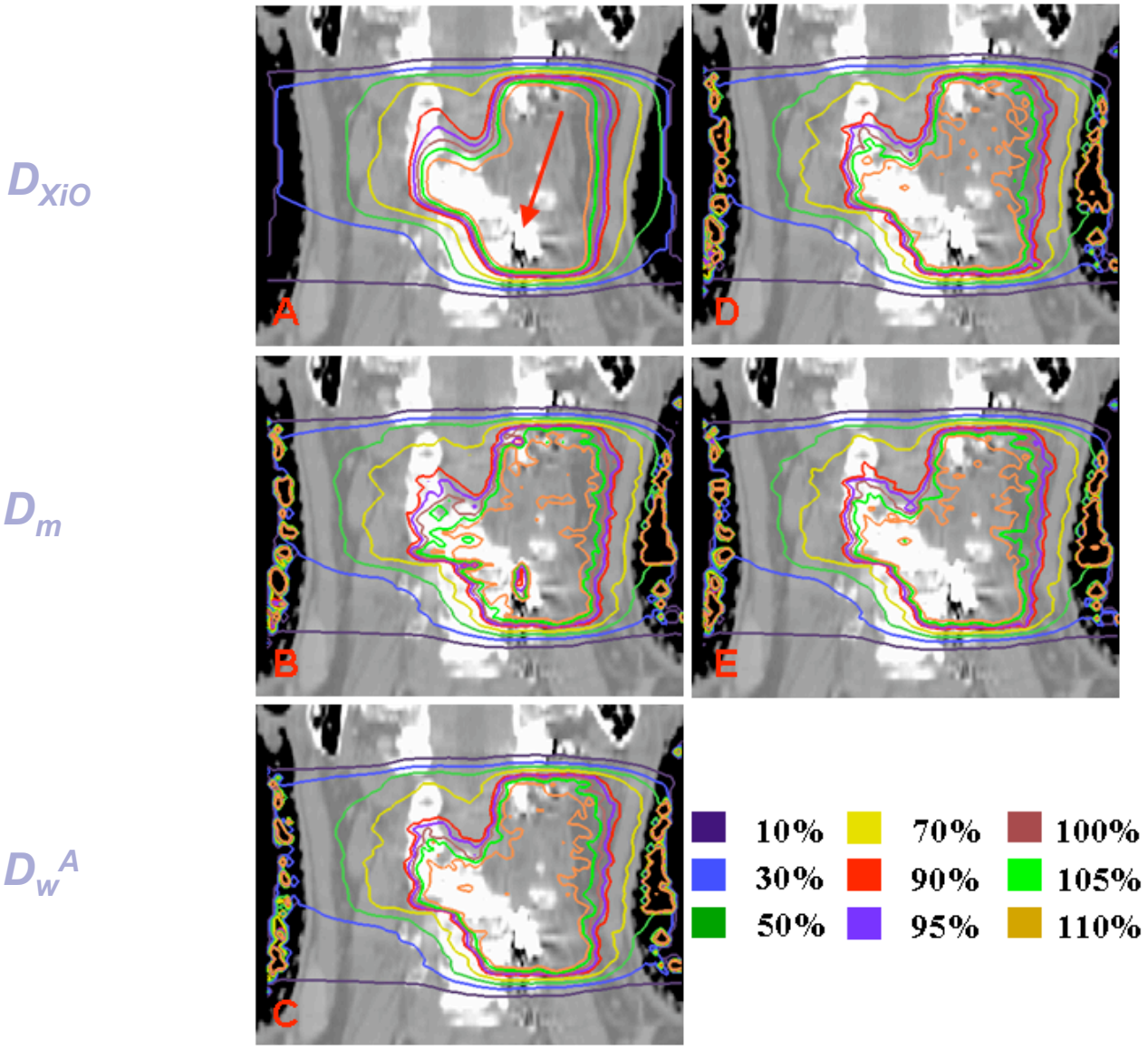

H. Paganetti, Phys. Med. Biol. 54, 2009

Dose-to-water versus Dose-to-tissue

- In general 3 conversion approaches for D_w agree within 1%
- Linear dependence of the relative D_w - D_m deviation with CT number (up to 10% in bony structures, negligible in soft tissue)

Dose-to-water D_w vs. dose-to-tissue D_m

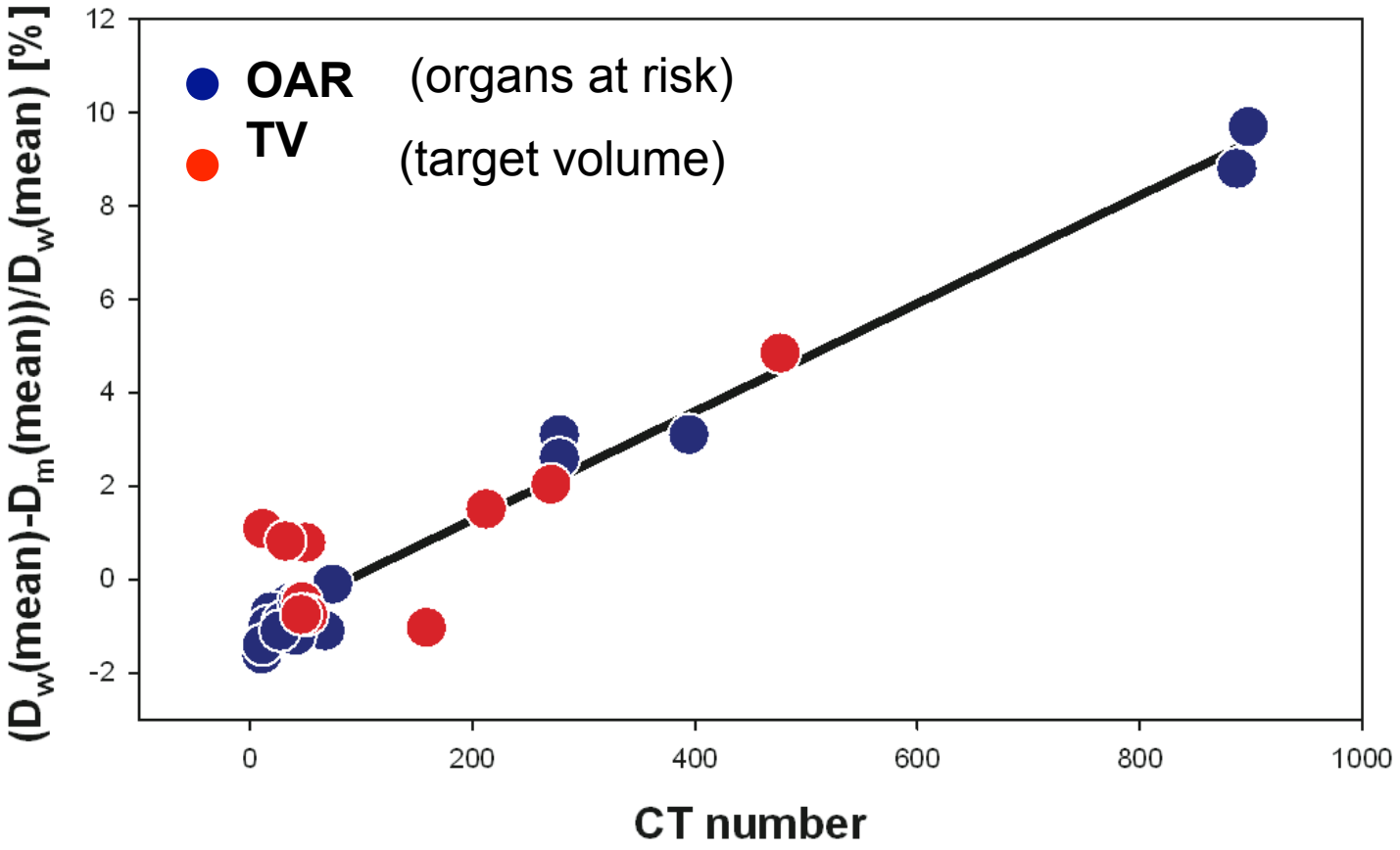

Paganetti, PMB 53, 2008

Biological basis of carbon beam therapy

Relative Biological Effectiveness

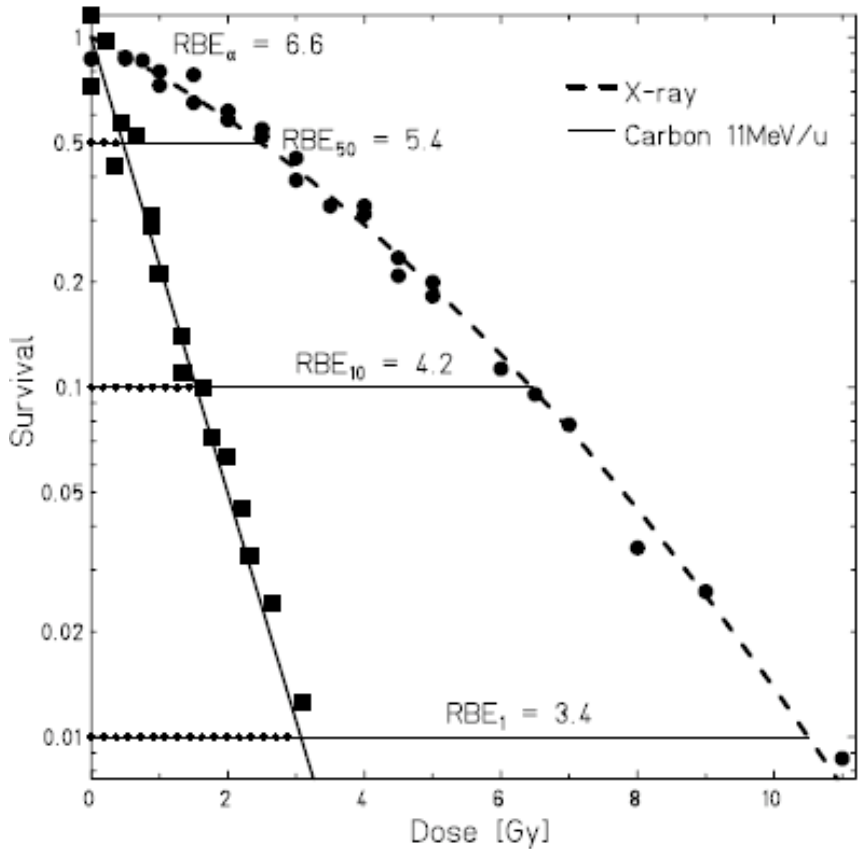

M. Krämer et al, Technology in Cancer Research & Treat., 2003

$$RBE = \frac{D_{Photon}}{D_{Ion}}\bigg|_{Isoeffect}$$

High LET particles (heavy ions) are more effective in cell killing than low LET radiation; this a consequence of their track structures, their energy deposition is restricted to small subvolumes along the particle trajectory.

The energy loss is partially transferred to the liberated electrons which are mostly ejected with low energy, leading to high ionization densities in the track center. Due to this high ionization density within the track, the damages are produced closed together resulting in a high amount of clustered DNA lesions mostly irreparable.

In clinical practice the RBE for protons is assumed to be 1.1.

Biological Monte Carlo calculations: FLUKA coupled with the Local Effect Model

Photon response **Microscopic dose distribution**

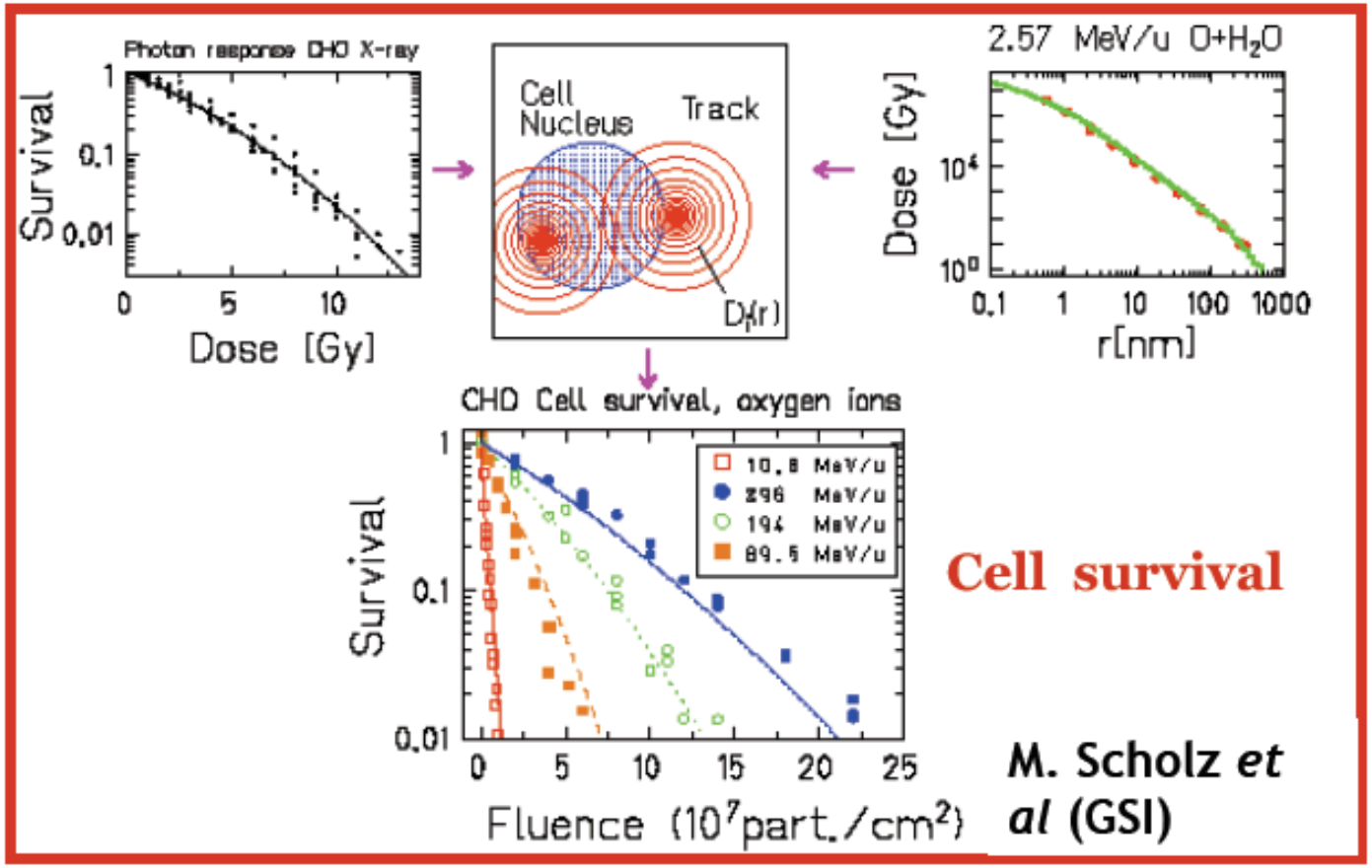

MC Biological Calculations in Carbon Ion Therapy

Benchmark in water against experimental data and analytical calculations

(A. Mairani PhD Thesis 2007)

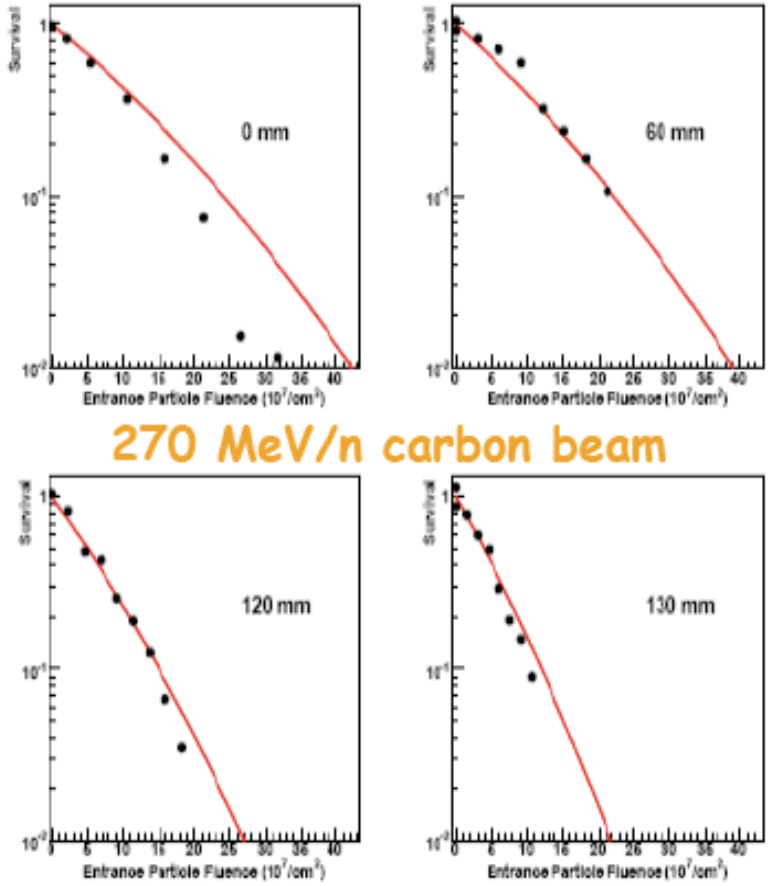

187 MeV/n carbon beam

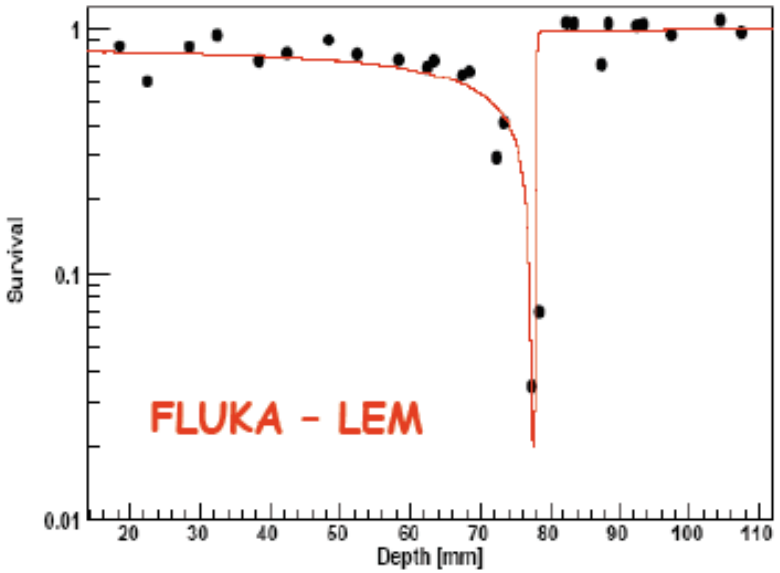

Exp. data (points)

Radiat. Environ. Biophys. 36 (1997) 59

MC Biological Calculations in Carbon Ion Therapy

FLUKA coupled with the LEM (*FLUKA-BIO*) has been used for a forward recalculation of a biologically optimized TRiP98 plan

Two-Dimensional Cell Survival Distributions

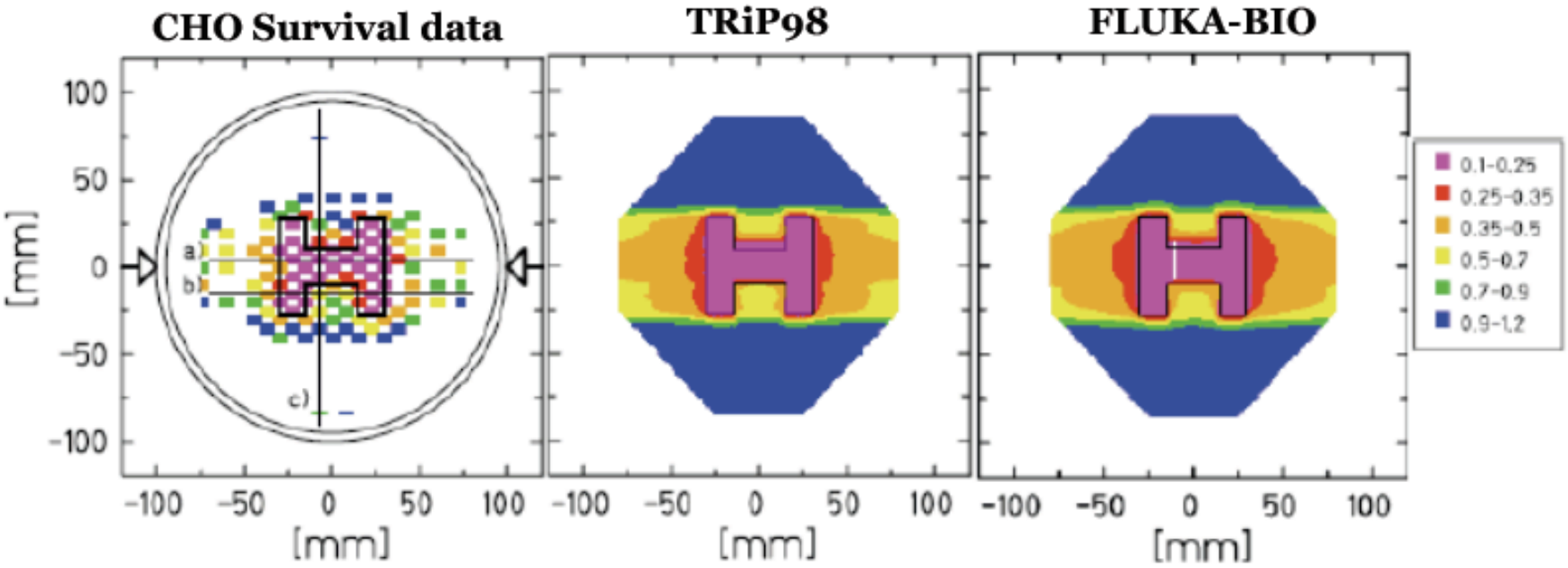

Exp. data and analytical calculations from M. Krämer *et al*, PMB 48 2003
Simulation: A. Mairani *et al* PMB *submitted*

MC Biological Calculations in Carbon Ion Therapy

FLUKA coupled with the LEM (*FLUKA-BIO*) has been used for a forward recalculation of a biologically optimized TRiP98 plan

One-Dimensional Cell Survival Distributions

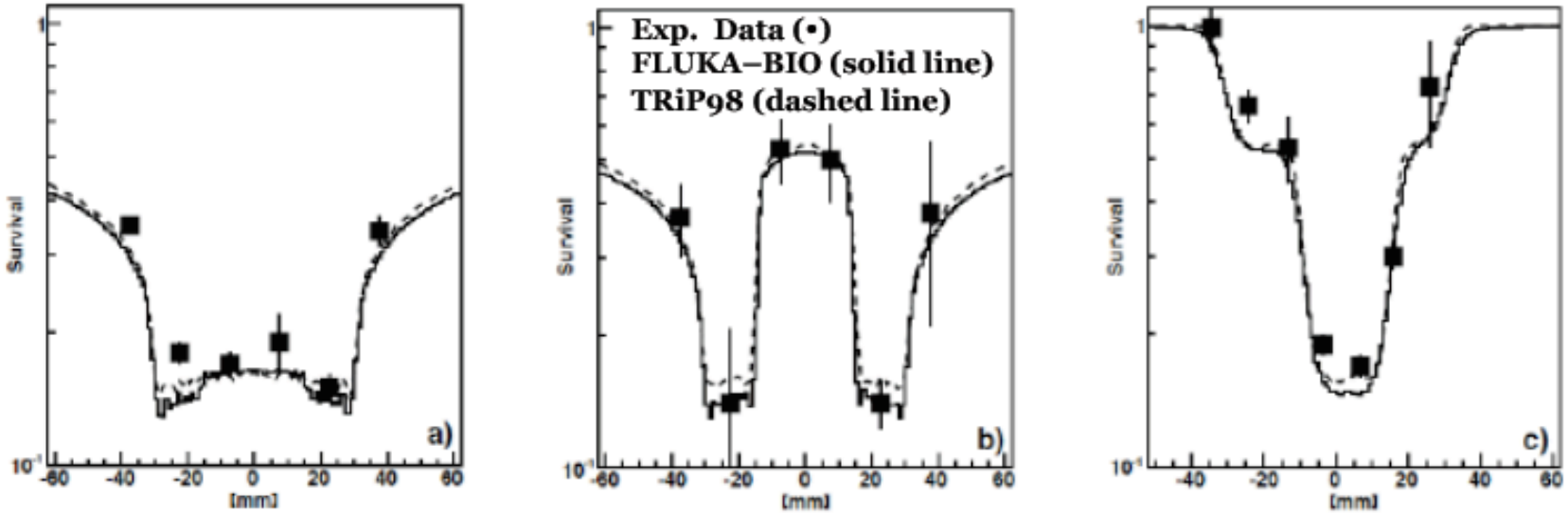

Exp. data and analytical calculations from M. Krämer *et al*, PMB 48 2003
Simulation: A. Mairani *et al* PMB *submitted*

Principle of PET

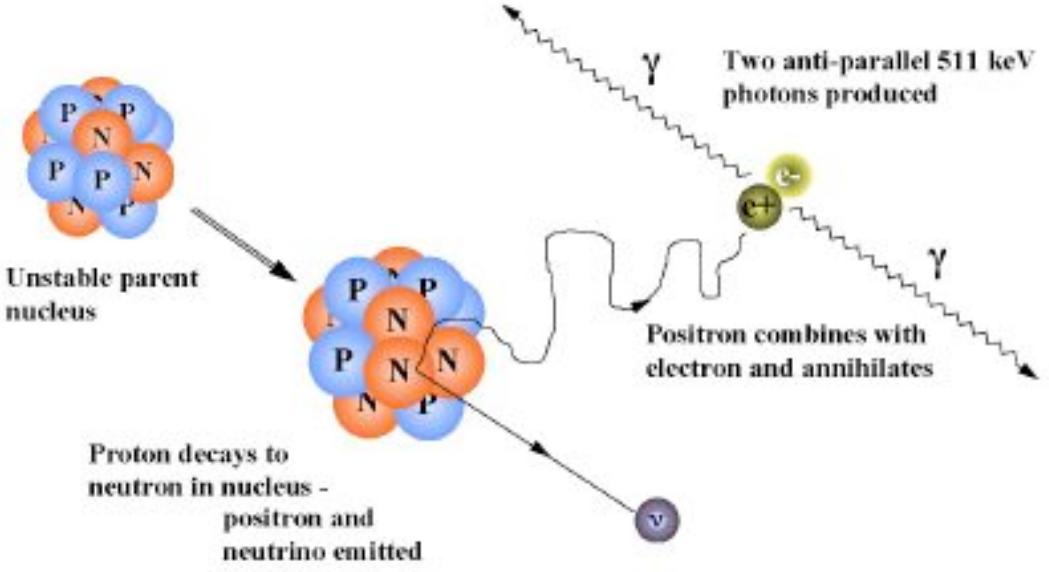

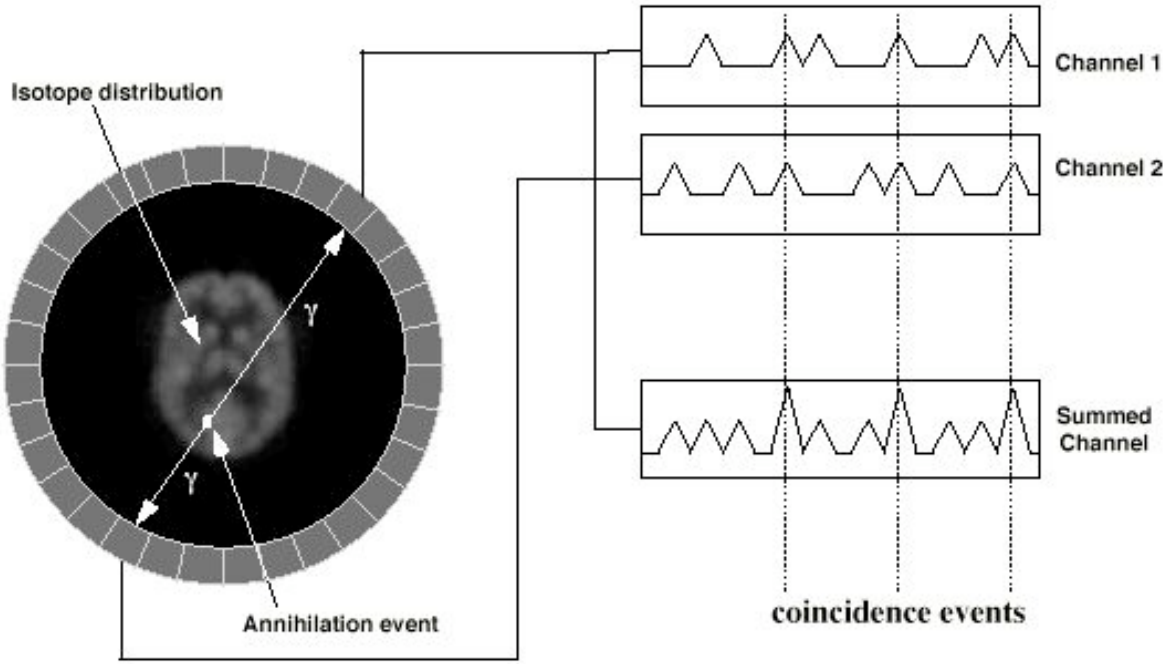

Range uncertainties issues in ion therapy

Difference TP / delivery

- Daily setup variations
- Internal organ motion
- Anatomical / physiological changes

Dose calculation errors

- Conversion *HU - ion range*
- CT artifacts

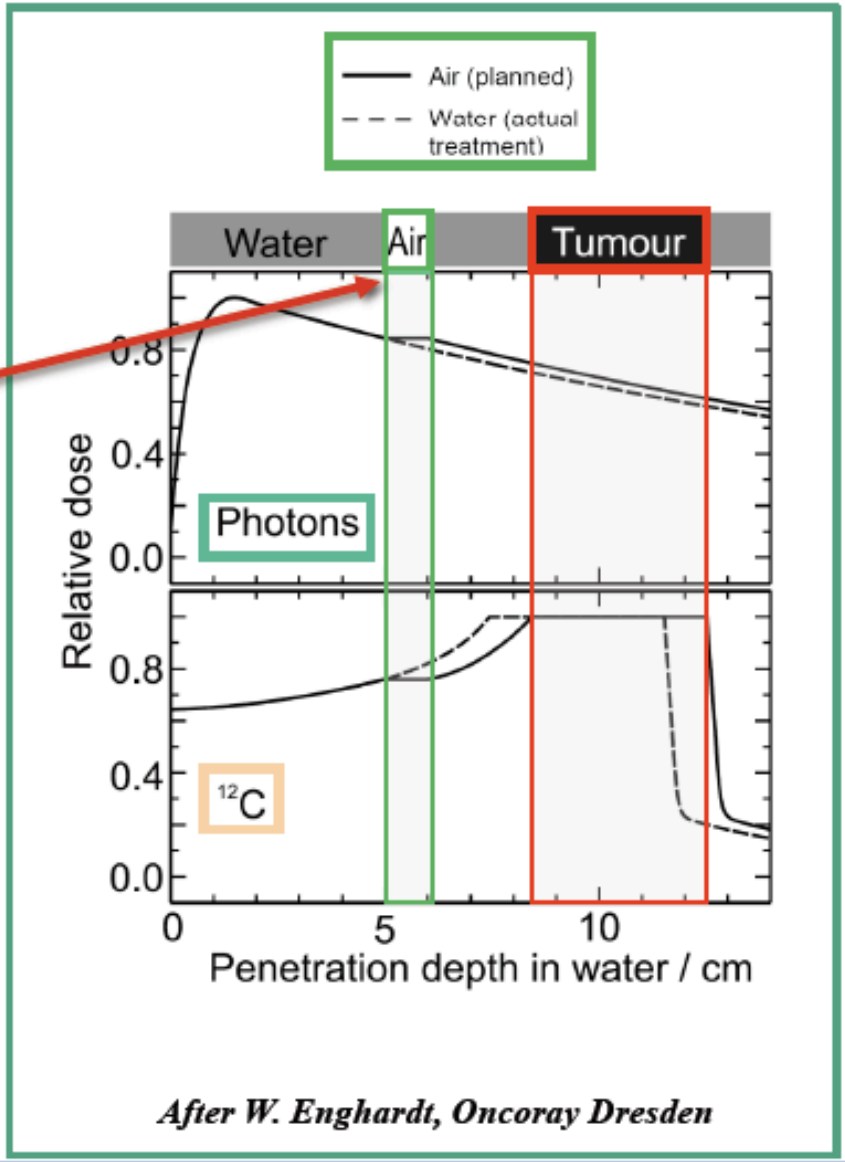

After W. Enghardt, Oncoray Dresden

The principle of PET verification

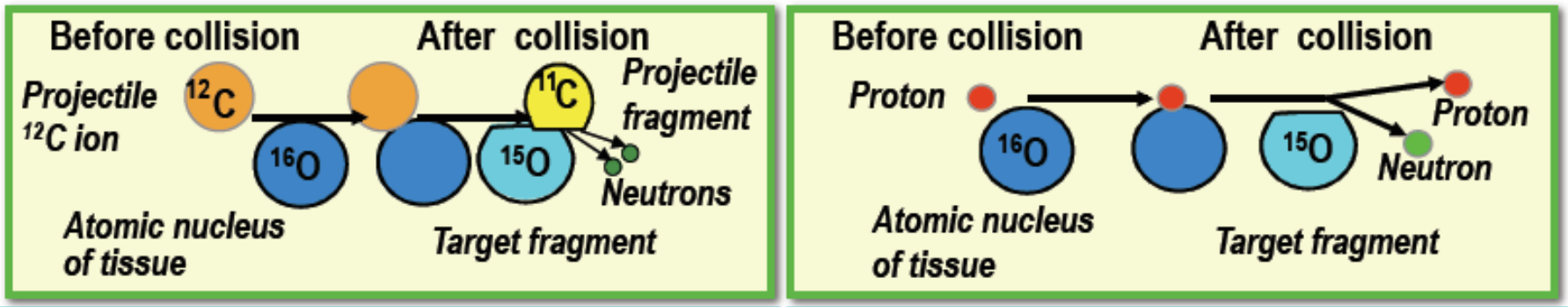

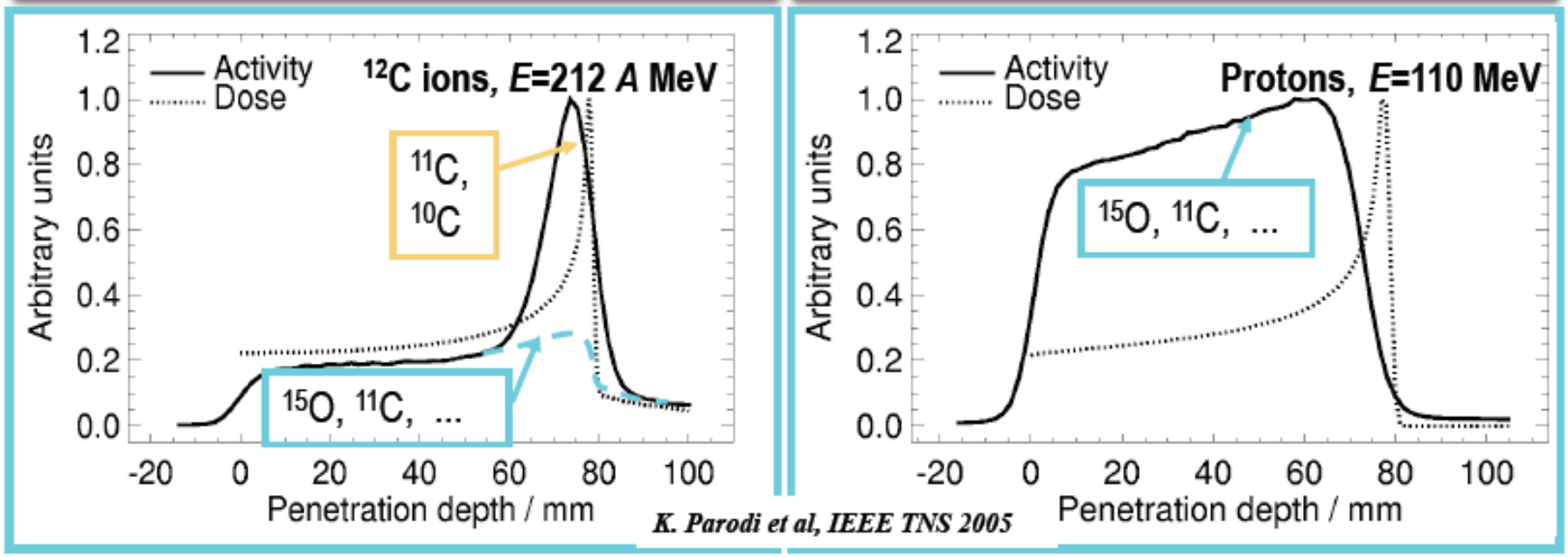

K. Parodi et al, IEEE TNS 2005

By-product of irradiation (^{15}O, ^{11}C, ^{13}N...with $T_{1/2}$ ~ 2, 20 and 10 min)

The principle of PET verification

A(r) ≠ D(r): "Dose-guidance„ from "surrogate„ PET ?

➔ ***Measured activity compared with calculation***

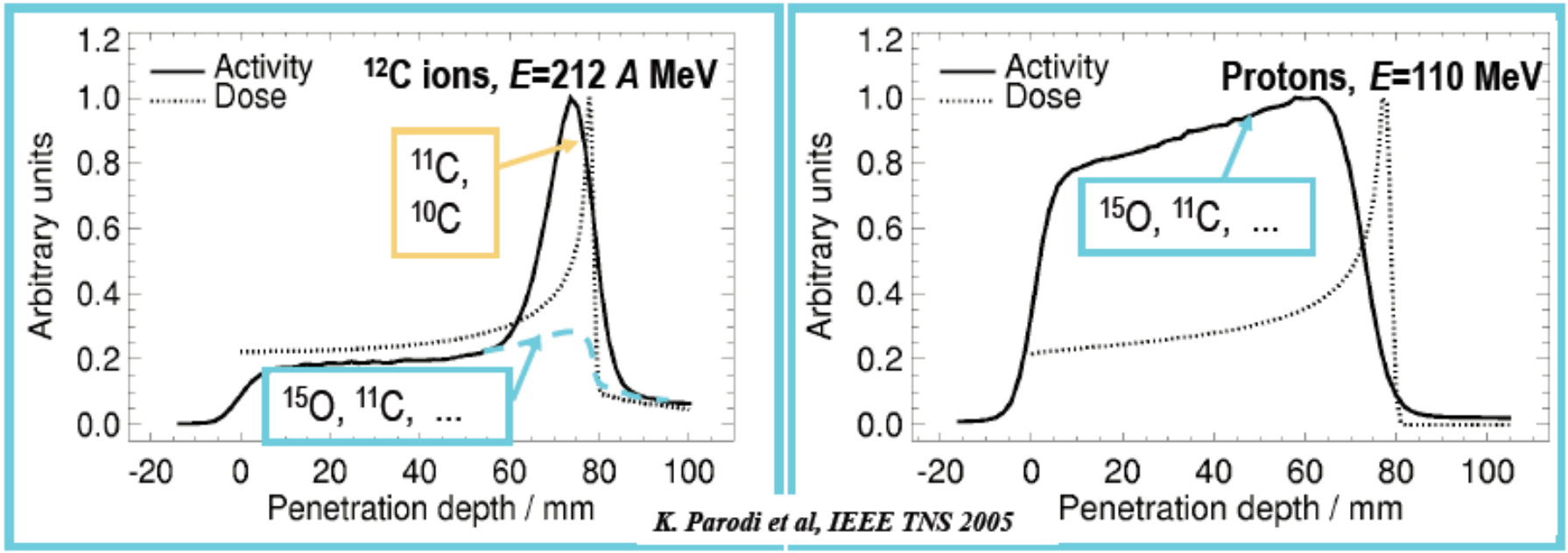

K. Parodi et al, IEEE TNS 2005

By-product of irradiation (^{15}O, ^{11}C, ^{13}N...with $T_{1/2}$ ~ 2, 20 and 10 min)

Calculation model of β^+ - activation

FLUKA Monte Carlo code using

- Field-specific beam source information from Geant4 modeling of the nozzle and beam modifiers ***(Paganetti et al, MP 31, 2004)***
- Planning CT (segmented into 27 material) and same CT-range calibration curve as TPS ***(Parodi et al MP 34, 2007, PMB 52, 2007)***
- Experimental cross-sections for β^+-emitter production
- Semi-empirical biological modeling ***(Parodi et al IJROBP 2007)***
- Convolution with 3D Gaussian kernel (7-7.5 mm FWHM)

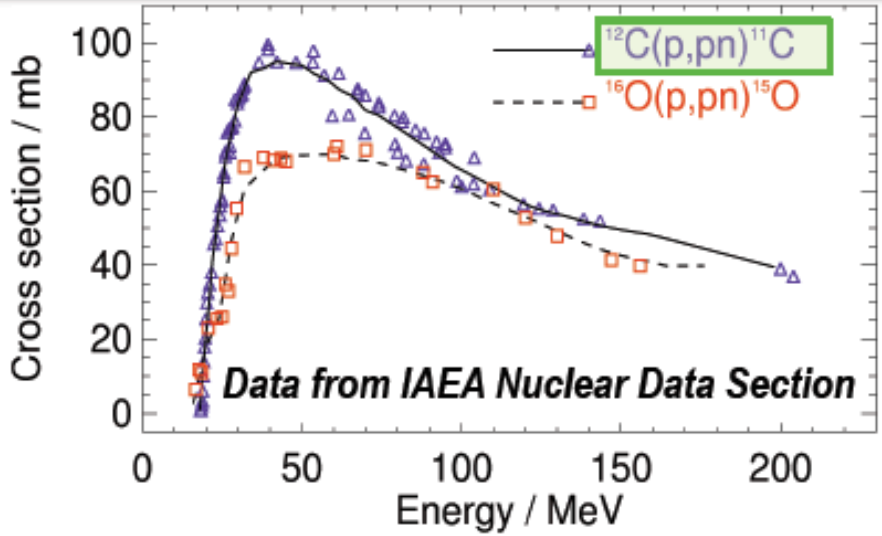

…and other reaction channels on N, O, Ca yielding, e.g., ^{13}N, ^{38}K, …

(Parodi et al, PMB 45, 2002, Parodi et al, PMB 52, 2007)

Parodi et al., IJROBP 68 2007

Clival Chordoma
Field 1: 0.87 Gy, $\Delta T_1 \sim 26$ min
Field 2: 0.87 Gy, $\Delta T_2 \sim 16$ min
PET $t_{meas} = 30$ min

The clinical study (skull base tumour)

TP Dose Calculation

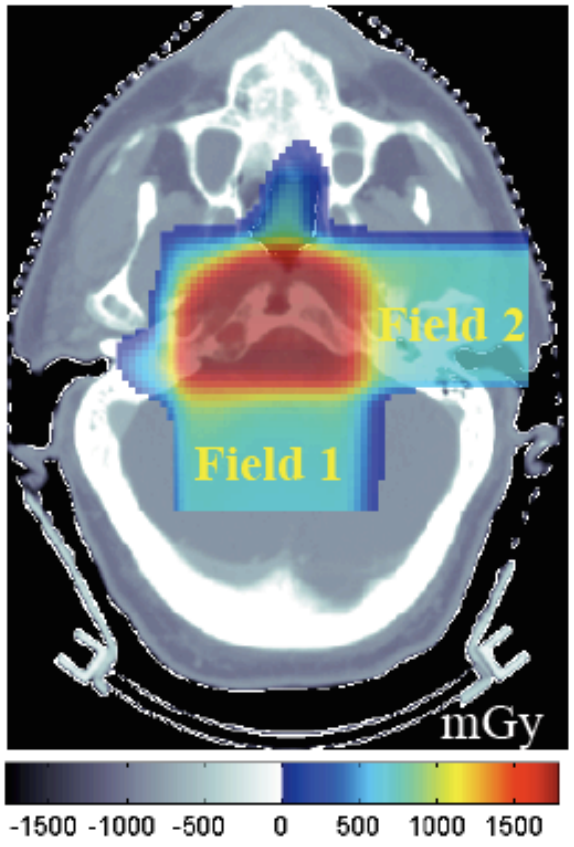

MC dose Calculation

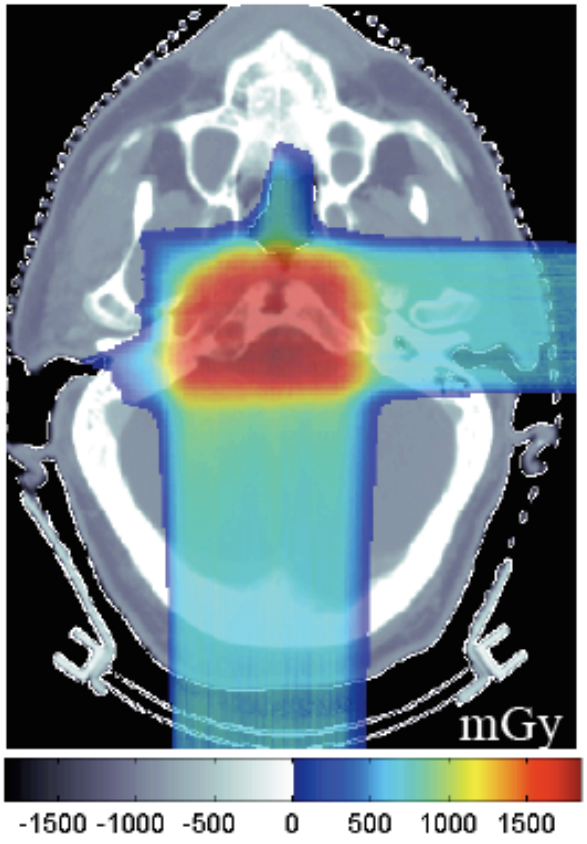

Parodi et al., IJROBP 68 2007

Clival Chordoma
Field 1: 0.87 Gy, $\Delta T_1 \sim 26$ min
Field 2: 0.87 Gy, $\Delta T_2 \sim 16$ min
PET $t_{meas} = 30$ min

The clinical study (skull base tumour)

TP Dose Calculation

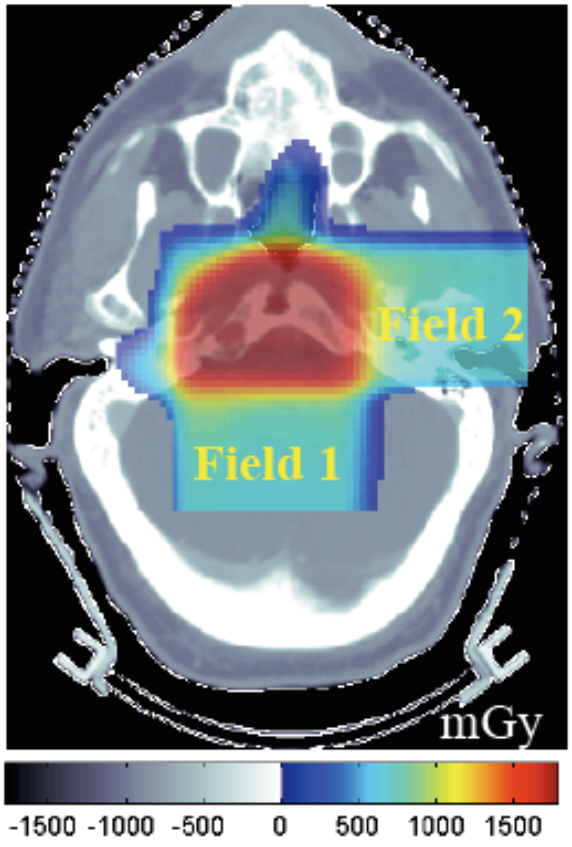

MC PET Calculation

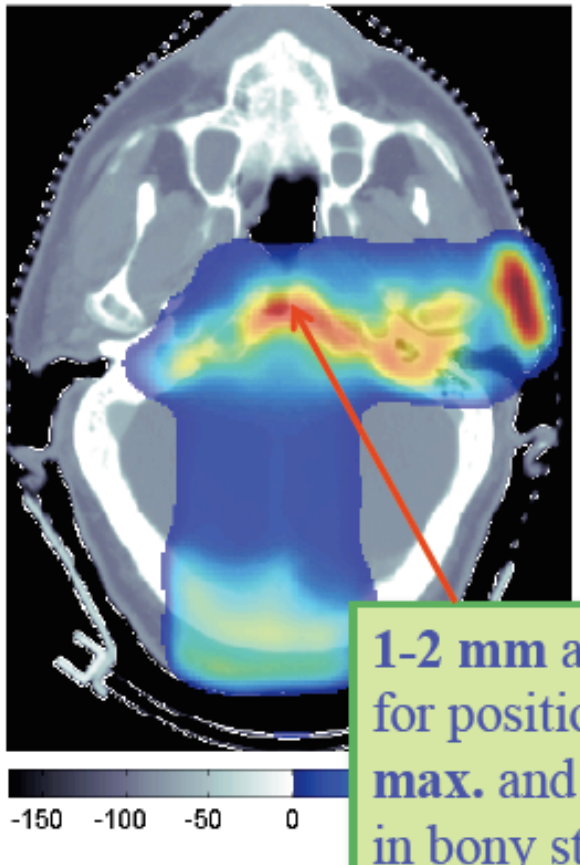

PET/CT Meas.

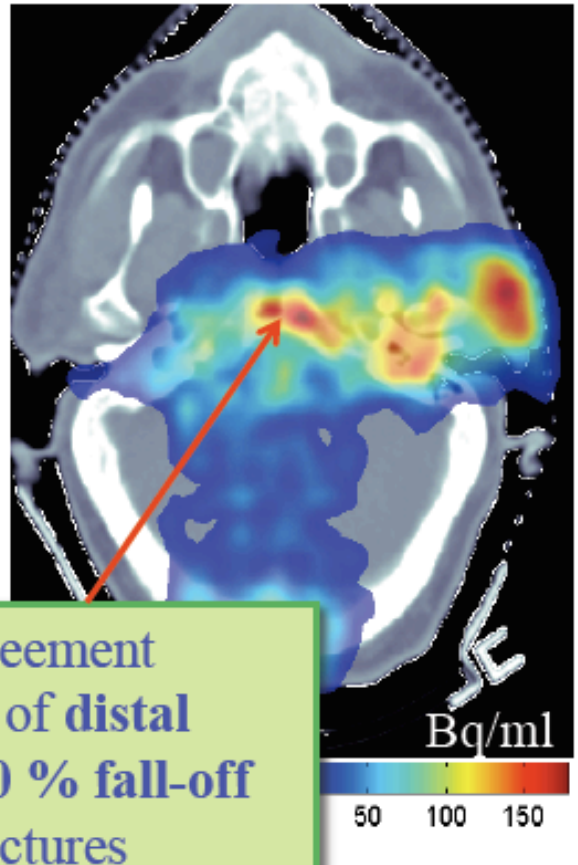

1-2 mm agreement for position of **distal max.** and **50 % fall-off** in bony structures

PET extension to in-beam PET of heavier ions

Ongoing work on:

- Application of FLUKA to PET monitoring of ions (e.g. ^{12}C, ^{16}O) based on internal nuclear models
- Simulation of imaging process (β^+-decay, propagation of e^+ and annihilation photons, detection) same as for measured data

F. Sommerer et al, PMB 54 2009

In-beam PET phantom experiments @ GSI

260 MeV/u ^{12}C ion on graphite, backprojections

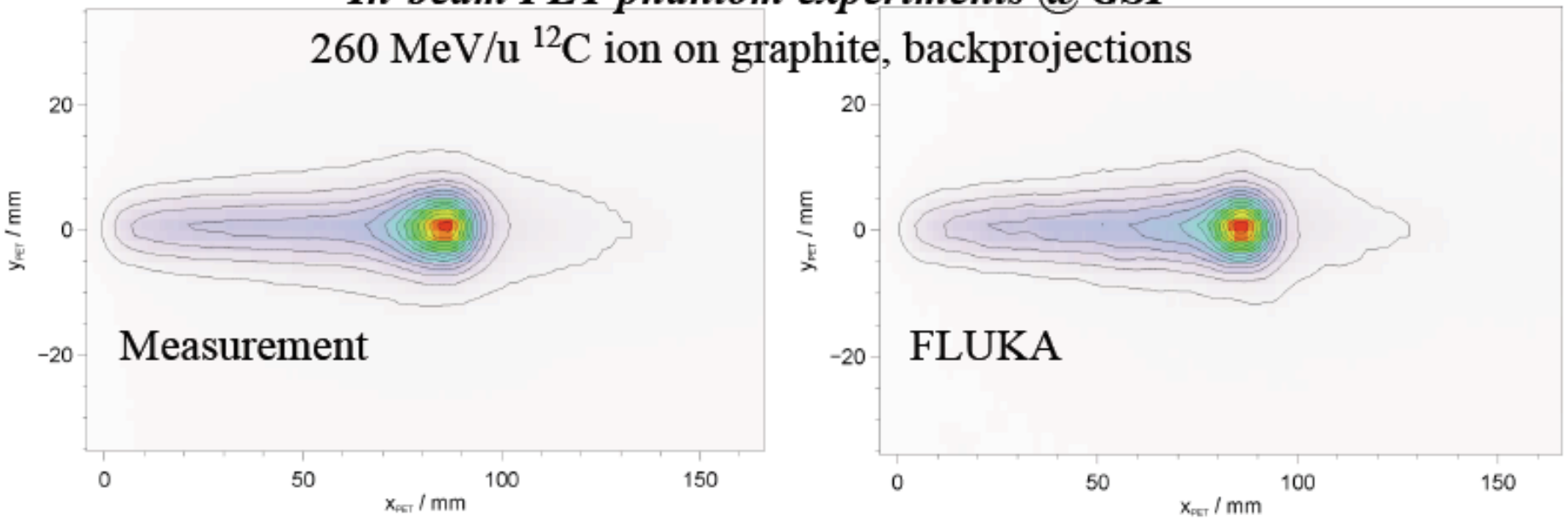

FLUKA – Dose distribution calculation in Nuclear Medicine applications

[eg: therapy with ^{131}I, ^{90}Y, ^{177}Lu labelled molecules]

Input:

CT image:
density map

+

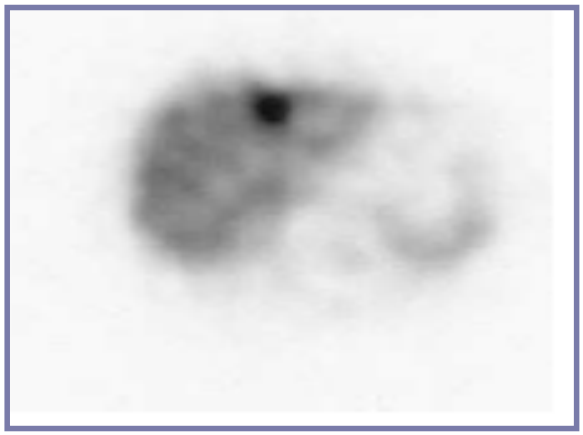

functional image (SPECT, PET):
activity distribution

Output:

- dose distribution (Gy/GBq, Gy) at voxel level
- Dose Volume Histogram [target tissue, healthy organs]

F. Botta (IEO) and A. Mairani (INFN)

Preliminary calculations:

Dose Point Kernel for low energy electrons [point isotropic source]

- **Monoenergetic electrons – 1 MeV**

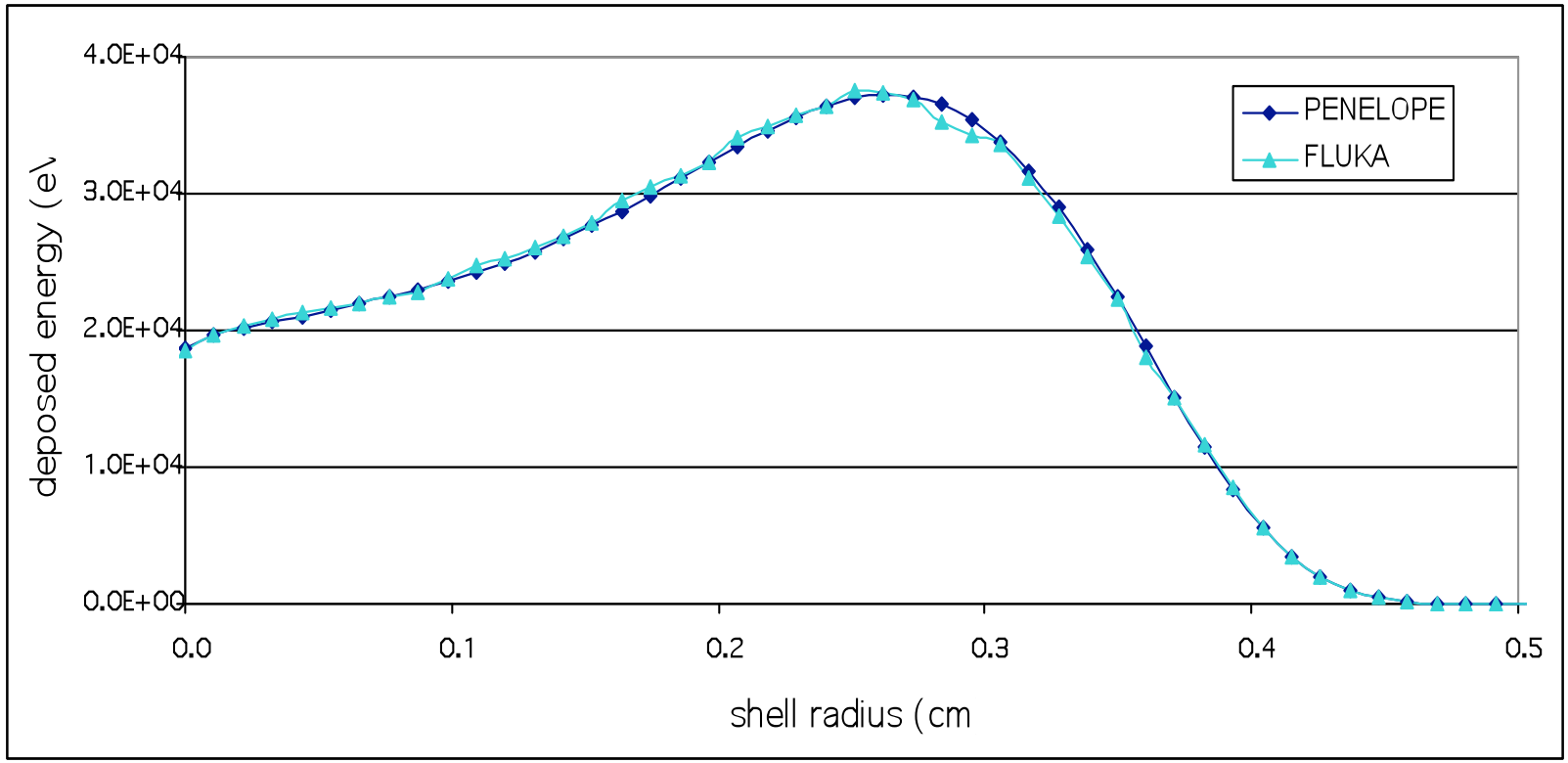

Preliminary calculations:

Dose in Anthropomorphic Phantom (example, ^{131}I in the lung)

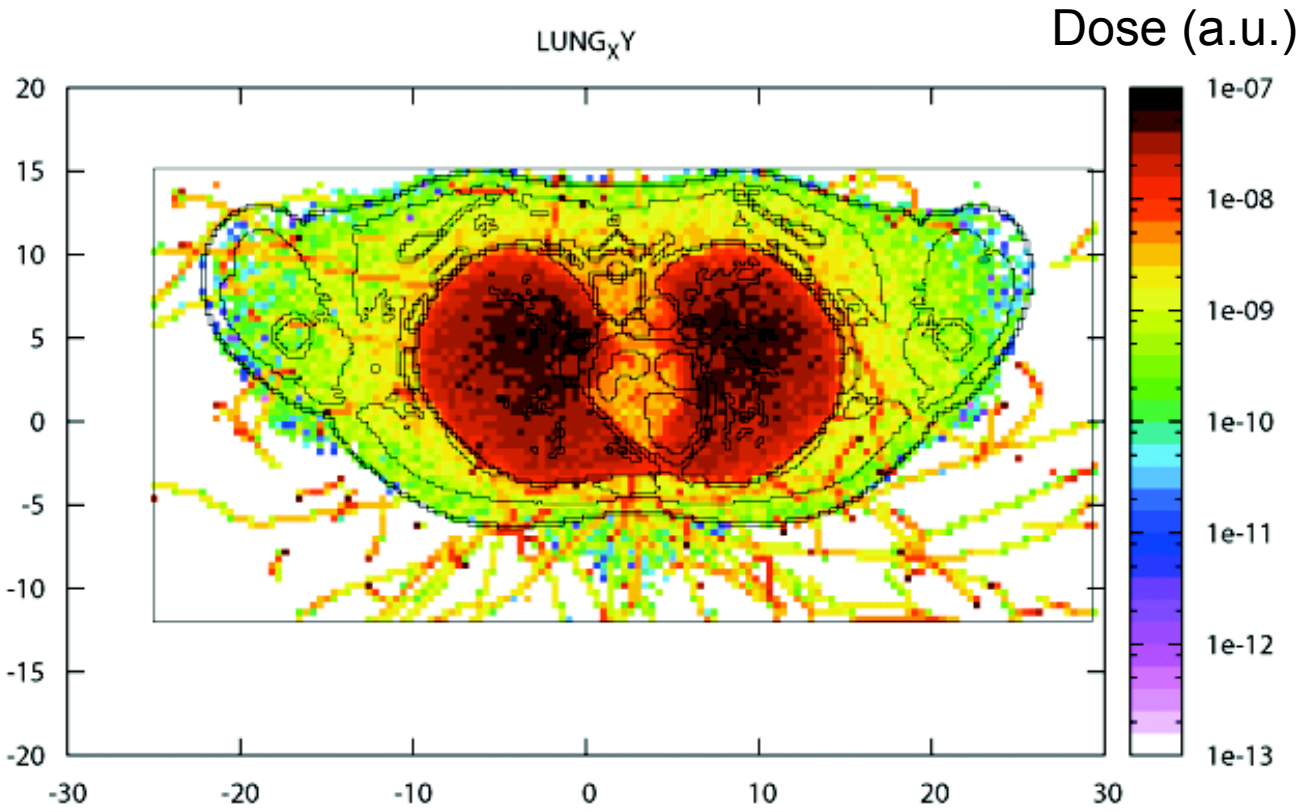

Material sources:

- "Advanced dosimetric concepts for radiation therapy"
  Dr K Parodi, Heidelberg, Germany

- FLUKA Course Material (www.fluka.org)

- Paolo Colleoni, Tesi Scuola di specializzazione in Fisica Sanitaria